Original Article

MOLECULAR METABOLISM

Novel translational mouse models of metabolic dysfunction-associated steatotic liver disease comparable to human MASLD with severe obesity

Katharina L. Hupa-Breier[1,*], Heiko Schenk[2], Alejandro Campos-Murguia[1], Freya Wellhöner[1], Benjamin Heidrich[1], Janine Dywicki[1], Björn Hartleben[3], Clara Böker[5], Julian Mall[5], Christoph Terkamp[1], Ludwig Wilkens[6], Friedrich Becker[4], Karl Lenhard Rudolph[4], Michael Peter Manns[1], Young-Seon Mederacke[1], Silke Marhenke[1], Hanna Redeker[1], Maren Lieber[1], Konstantinos Iordanidis[1], Richard Taubert[1], Heiner Wedemeyer[1], Fatih Noyan[1], Matthias Hardtke-Wolenski[1,7,9], Elmar Jaeckel[1,8,9]

ABSTRACT

Objective: Metabolic dysfunction-associated steatotic liver disease (MASLD) is the most common cause of chronic liver disease, especially in patients with severe obesity. However, current mouse models for MASLD do not reflect the polygenetic background nor the metabolic changes in this population. Therefore, we investigated two novel mouse models of MASLD with a polygenetic background for the metabolic syndrome.
Methods: TALLYHO/JngJ mice and NONcNZO10/LtJ mice were fed a high-fat- high-carbohydrate (HF-HC) diet with a surplus of cholesterol diet. A second group of TH mice was additional treated with empagliflozin.
Results: After sixteen weeks of feeding, both strains developed metabolic syndrome with severe obesity and histological manifestation of steatohepatitis, which was associated with significantly increased intrahepatic $CD8^+$cells, $CD4^+$cells and Tregs, contributing to a significant increase in pro-inflammatory and pro-fibrotic gene activation as well as ER stress and oxidative stress. In comparison with the human transcriptomic signature, we could demonstrate a good metabolic similarity, especially for the TH mouse model. Furthermore, TH mice also developed signs of kidney injury as an extrahepatic comorbidity of MASLD. Additional treatment with empagliflozin in TH mice attenuates hepatic steatosis and improves histological manifestation of MASH.
Conclusions: Overall, we have developed two promising new mouse models that are suitable for preclinical studies of MASLD as they recapitulate most of the key features of MASLD.

Keywords Metabolic dysfunction-associated steatotic liver disease; Metabolic syndrome; Mouse model; Kidney injury; Non-alcoholic fatty liver disease

[1]Department of Gastroenterology, Hepatology, Infectious Diseases and Endocrinology, Hannover Medical School, Hannover, Germany [2]Department of Nephrology and Hypertension, Hannover Medical School, Hannover, Germany [3]Institute of Pathology, Hannover Medical School, Hannover, Germany [4]Research Group on Stem Cell and Metabolism Aging, Leibniz Institute on Aging - Fritz Lipmann Institute (FLI), 07745, Jena, Germany [5]Department of General, Visceral, Vascular and Bariatric Surgery, Klinikum Nordstadt, 30167, Hannover, Germany [6]Department of Pathology, Nordstadt Hospital Hannover, 30167, Hannover, Germany [7]Institute of Medical Microbiology, University Hospital Essen, University Duisburg-Essen, Essen, Germany [8]Ajmera Transplant Centre, Toronto General Hospital, United Health Network, University of Toronto, Toronto, Canada

[9] Matthias Hardtke-Wolenski and Elmar Jaeckel contributed equally to this work.

*Corresponding author. Department of Gastroenterology, Hepatology, Infectious Diseases and Endocrinology, Hannover Medical School, Carl-Neuberg-Str. 1, 30625, Hannover, Germany. E-mail: hupa.katharina@mh-hannover.de (K.L. Hupa-Breier).

Abbreviations: ALT, alanine aminotransferase; AST, aspartate aminotransferase; BAT, brown adipose tissue; ER, endoplasmatic reticulum; FACS, fluorescence-activated cell sorting; GLP-1, Glucagon-like peptide 1; HE, Hematoxylin- Eosin; HF-HC, high-fat- high-carbohydrate; HOMA-IR, Homeostasis Model Assessment for insulin resistance; IPGTT, intraperitoneal glucose tolerance test; MASLD, Metabolic dysfunction-associated steatotic liver disease; MetS, metabolic syndrome; MoMF, monocyte-derived macrophages; NAFL, non-alcoholic fatty liver; NAFLD, Non-alcoholic fatty liver disease; NAS, NAFLD-activity score; NASH, Non-alcoholic steatohepatitis; NCD, normal chow diet; NGAL, Neutrophil Gelatinase Associated Lipocalin; nNZO10, NONcNZO10Lt/J mice; PAS, Periodic-acid Schiff reaction; SGLT-2, sodium-glucose transport protein-2; T2DM, type 2 diabetes mellitus; TH, TALLYHO/JngJ; KIM-1, Urinary kidney injury molecule-1; VAT, visceral adipose tissue; WAT, white adipose tissue

Received November 27, 2024 • Revision received January 21, 2025 • Accepted January 21, 2025 • Available online 22 January 2025

https://doi.org/10.1016/j.molmet.2025.102104

1. INTRODUCTION

Metabolic dysfunction-associated steatotic liver disease (MASLD), formerly known as non-alcoholic fatty liver disease (NAFLD), is the most common liver disease worldwide, affecting nearly 38% of the global adult population [1,2]. The metabolic syndrome (MetS), including central obesity, dyslipidemia, and type 2 diabetes mellitus (T2DM) plays a central role its pathogenesis [3]. Therefore, the concept of steatotic liver diseases (SLD) has been updated recently by the new concept of MASLD, which requires at least one out of five cardiometabolic risk factors in addition to hepatic steatosis [4]. In contrast to the old definition of NAFLD, which was defined by hepatic steatosis in the absence of any other liver disease, this new concept highlights the central role of metabolic dysfunction in the pathogenesis of MASLD. In particular, obesity is a major driver of MASLD. The overload of metabolic substrates in the liver leads to hepatic and peripheral insulin resistance followed by impaired lipid metabolism. Exhaustion of lipid metabolism is then causing oxidative stress and stress of the endoplasmatic reticulum followed by activation of pro-inflammatory pathways [5]. Furthermore, obesity also increases both the overall- and liver-related mortality in patients with MASLD [6,7].

However, current mouse models are mainly based on either monogenetic-modified mouse strains or dietary modifications and do neither represent the polygenetic background nor the metabolic changes of the metabolic syndrome, especially with severe obesity [8]. For further research in the field of MASLD, sufficient mouse models that represent the underlying metabolic dysfunction of MASLD are crucial.

The NONcNZO10Lt/J strain is a polygenetic mouse model for type 2 diabetes as male mice develop obesity, hyperinsulinemia and insulin resistance in liver and skeletal muscle [9]. The TALLYHO/JngJ strain also mimics many features of the human non-insulin dependent type 2 diabetes. Female mice develop moderate obesity, hyperlipidemia and hyperinsulinemia [10]. Different whole genome analyses of obese type 2 diabetic mice revealed a complete catalogue of gene variants responsible for different features of the metabolic syndrome and type 2 diabetes [11]. In conclusion, both mice models display the polygenetic phenotype of the metabolic syndrome and therefore may be suitable for a MASLD mouse model.

Overnutrition as another key factor in the pathogenesis of MASLD has been addressed by several diets. Most successful diets combine a high fat, high carbohydrate diet with a surplus of cholesterol and fructose to achieve the histopathological features of MASLD [8].

In this study, we combine mouse models with a polygenetic background for obesity and metabolic syndrome with the high-fat-high carbohydrate diet with a surplus of cholesterol and fructose to obtain a mouse model for MASLD that mirrors the human pathogenesis of MASLD.

So far, weight loss is the most important treatment according to the current guidelines [12]. Furthermore, improvement of glycemic control could also improve disease activity independent of weight loss [13]. Inhibitors of the sodium-glucose cotransporter 2 (SGLT2i) such as empagliflozin are very effective anti-diabetic treatment. Their inhibition of the renal SGLT2-transporter prevents renal glucose reabsorption and thereby improves glucotoxicity [14,15]. The role of SGLT2i in MASLD is still under debate. On the one hand, a previous study showed reduction in liver fat content in patient with well-controlled diabetes and moderate obesity [16]. Furthermore, two recent studies could proof beneficial effects in patients with diabetes and MASLD, but without severe obesity [17,18]. However, the detailed pathophysiological pathways are not fully understood yet. In contrast, another large database study could not show beneficial effect of SGLT2i on liver related outcomes [19]. Therefore, we aimed to investigate the SGLT2i empagliflozin in the last step of developing a suitable mouse model of MASLD and obesity.

2. MATERIAL AND METHODS

2.1. Ethics statement

All animal experiments were executed according to protocols approved by the animal welfare commission of the Hannover Medical School and local Ethics Animal Review Board (Niedersaechsisches Landesamt für Verbraucherschutz und Lebensmittelsicherheit/LAVES, Oldenburg, Germany) covered by study number 17/2456 and are in accordance to the ARRIVE guidelines.

Human study was conducted at the Nordstadt Krankenhaus Hannover and at Hannvoer Medical School and approved by the local Ethic committee (Nr.8244_B0_S_2019, German Clinical Trial Register ID DRKS00017085). The study was performed in accord with the Declaration of Helsinki. All patients gave their written informed consent for data analyses.

2.2. Animals

We used female mice from TALLYHO/JngJ (TH; $n = 4$) and male NONcNZO10/LtJ (nNZO10; $n = 4$) strain. Starting at the age of 4 weeks, mice were fed with a high fat-high carbohydrate (HF-HC) diet with a surplus of cholesterol (Ssniff EF R/M D12330 mod.*/surwit + 1%Cholesterol; Diet#: E15771−34, S3542-E005) with 45 g/L 55 %Fructose/45 %Sucrose (Sigma) in the drinking water for 16 weeks. Control group mice were fed with a normal chow diet (NCD) from ssniff (Altromin standard diet # 1324 TPF, Altromin).

Additional to the first part, we conducted another experimental set-up to test SGLT2i empagliflozin. Therefore, mice received empagliflozin p.o. (225mg/kg diet) ($n = 8$) or regular HF-HC diet as control ($n = 7$) after 12 weeks of HF-HD diet for another for 4 weeks. All mice were sacrificed after 16 weeks of diet. Detailed protocols are listed in the supplementary.

2.3. Adipose tissue

Adipose tissue was extracted after dissection and weighed. Brown adipose tissue (BAT) was defined as interscapula adipose tissue, white adipose tissue (WAT) as gluteal adipose tissue and visceral adipose tissue (VAT) as the epididymal adipose tissue [20].

2.4. Intraperitoneal glucose-tolerance test

After 16 weeks of HF-HC diet, an intraperitoneal glucose-tolerance test (IPGTT) was performed. After 12 h of fasting, fasting blood glucose levels were measured (One Touch Ultra, LifeScan). Following this, 1 mg glucose/g bodyweight was administered and blood glucose levels were measured at 30, 60, 90 and 120 min after injection.

2.5. Serum analysis

Blood samples have been collected via a retro orbital withdrawal. Aspartate aminotransferase (AST), alanine transaminase (ALT), serum-triglycerides, cholesterol and serum-glucose in the blood were determined by photometric enzyme activity assays by the Olympus AU400 Chemistry Analyzer (OLY-AU400) using 40−50 µl of murine serum as described before [21]. DeRitis Quotient was calculated as followed: AST/ALT. Serum-Insulin was measured using the Ultra sensitive Mouse Insulin Elisa kit (Crystal Chem, Cat: 90080) in accordance to the manufacture guidelines. HOMA-IR (Homeostasis Model Assessment for insulin resistance) was calculated as previously described, using the equation: (fasting glucose [mg/dl] × fasting insulin [µIU/ml])/405) [22].

2.6. Liver triglycerides

Frozen liver was homogenized in 1x standard diluent (Cayman) with 20 μg/ml Leupeptin (Serva Electrophoresis GmbH) via a rod-homogenizer for 10—15s. Homogenates were centrifuged at 4 °C for 10 min at 10.000g. Supernatant was aliquoted for triglyceride and protein quantification. Colorimetric detection and quantitation of total protein was done using the Pierce™ BCA Protein Assay Kit (Thermo-FisherScientific). Triglyceride in supernatant was detected via the Cobas® 8000 modular analyzer (HITACHI/Roche).

2.7. Liver histology

Murine liver was fixed in formalin, embedded in paraffin and prepared for Hematoxylin- Eosin, Periodic-acid Schiff reaction (PAS) and silver staining. Afterwards, they were graded for the NAFLD-activity score (NAS) [23] by blinded pathologist. Sirius Red staining of paraffin-embedded liver sections was performed according to the manufacturer's protocol (Sigma—Aldrich) and quantified by analyzing four microscopic fields at a 100-fold magnification (Olympus BX 51) with Fiji [24]. Quantification of hepatic hydroxyproline content was prepared as described before [25].

2.8. Flow cytometry

Livers and spleens were perfused and dissected from mice. Organs were minced using nylon cell strainer (70 μm, BD Falcon) and washed with phosphate-buffered saline supplemented with 2% fetal calf serum. Afterwards, spleens were subjected to red blood cell lysis puffer (Sigma). Intrahepatic leucocytes and monocytes were isolated by using 40%/70%- Percoll density gradients (Percoll, GE Healthcare). Afterwards, all cells were stained with fluorochrome-conjugates antibodies for multicolor flow cytometry analysis (see Suppl). All acquisitions were done with a LSRII SORP interfaced to DIVA software (BD Biosciences).

2.9. Real-time PCR

For Real-time PCR we used the TaqMan Gene Expression Assay. For amplification, we used the PreAmp master Mix (Fluidigm, PN 100—5580) according to the manufacture guidelines (Real-Time PCR user guide for the Fast gene Expression Analysis using TaqMan gene Expressions Assays). For PCR, we used the 48.48 Dynamic Array ™ IFC, Assay loading reagent (Fluidigm, PN 85000736), GE Sample Loading Reagent (Fluidigm, PN 85000735, 85000746) and the Master Mix (TaqMan Gene Expression Master Mic, Applied Bioscience, PN 4369016) according to the manufactures guidelines.

2.10. Proteomics analysis

Detailed prescription of liver proteomic analyses is provided in the Supplementary. Preparation and analyses were performed by the Proteomics Core facility at the Leibniz Institute on Aging, Jena.

2.11. Kidney qPCR

Purification of total RNA from mouse kidneys was performed by using the RNeasy Plus Mini Kit (Qiagen, Hilden, Germany) according to the manufacture's protocol. Reverse transcription of RNA was done using Oligo(dT)primer (Promega, Madison, WI, USA), and Random primers (Promega, Madison, WI, USA) that were incubated at 70 °C for 10min followed by retrotranscription in M-MLV RT buffer (Promega, Madison, WI, USA), with dNTPs (Roche, Mannheim, Germany), and M-MLV reverse transcriptase (Promega, Madison, WI, USA) at 42 °C for 90min and at 70 °C for 10min. Sybr green-based qPCR was carried out using the TaKaRa SYBR Premix Ex TaqTMII (Takara Bio Europe SAS, Saint-Germain-en-Laye, France) (See Suppl.).

2.12. Stool analysis

Fresh stool was collected from TH after 16weeks of diet before dissection. DNA preparation and bioinformatical analysis were performed according to the methods described before [26].

2.13. Human BulkRNA sequencing

Human liver samples were collected from obese patients, who received bariatric surgery. We analyzed samples from patients with severe obesity and histological proven MASH (NAS$<$3) ($n = 7$) compared to patients with severe obesity and no histological signs of steatosis or MASLD ($n = 6$). BulkRNA sequencing was performed at BGI Genomics. Detailed information are presented in the supplementary.

2.14. Statistics

Statistical analysis and graphical presentations were performed with Prism 5.01 and Prism 8.2.1 (GraphPad).

The unpaired Student 2-tailed t-test, if necessary with Welsh correction was applied for comparisons of two groups. Non-parametric Mann—Whitney test was used for comparing the medians of NAS. The trapezoidal rule was used to determine the area under the curve (AUC). P-values <0.05 were considered as significant. All results were presented with mean and standard deviations (SD).

For analysis of the RT-PCR, we used the Fluidigm Real-Time PCR Analysis Software V.3.0.2. For normalization we subtracted the mean values of the housekeeping genes glyceraldehyde-3-phosphate dehydrogenase (Gapdh) and actin beta (actb) from the genes of interest. Heat map and PCA analysis of the −delta Ct values were plotted via the Qlcore software ($p < 0.05$ and $q < 0.2$). P-values <0.05 were considered as significant. All results were presented with mean and standard deviation (SD).

$^{*}P < 0.05$; $^{**}P < 0.01$; $^{***}P < 0.001$ was used for comparison of TH, NCD vs TH, HF-HC

$^{+}P < 0.05$; $^{++}P < 0.01$; $^{+++}P < 0.001$ was used for comparison of nNZO10, NCD vs nNZO10, HF-HC

A p-value >0.05 was considered as not significant (ns).

3. RESULTS

3.1. Both strains develop marked features of the metabolic syndrome

As obesity is an important aspect of the metabolic syndrome, we characterised the body composition after 16 weeks of HF-HC. nNZO10 mice gained weight and developed obesity (Figure 1B) with a significant increase in white and brown adipose tissue (Supplementary Figure 1A). TH already develop central obesity under NCD. Under HF-HD diet, they develop only a slight weight gain ($p = 0.06$), without a significant increase in WAT, VAT and BAT mass.

Both strains developed hyperglycemia after 16 weeks of HF-HC diet with significantly increased AUC (Figure 1C). As a marker for insulin resistance, we measured insulin after fasting period and calculated the HOMA-IR (Supplementary Figure S1B). Here, we could show that nNZO10 developed insulin resistance after HF-HC diet. Furthermore, serum cholesterol levels increased in nNZO and TH mice (Supplementary Figure S1C) after HF-HC diet.

In summary, both strains developed central obesity, hyperglycemia and dyslipidemia as key aspects of the metabolic syndrome.

3.2. Serological development of hepatitis

Elevated levels of AST and ALT are serological signs of hepatitis. While elevated AST levels were observed in TH and nNZO mice, the latter also

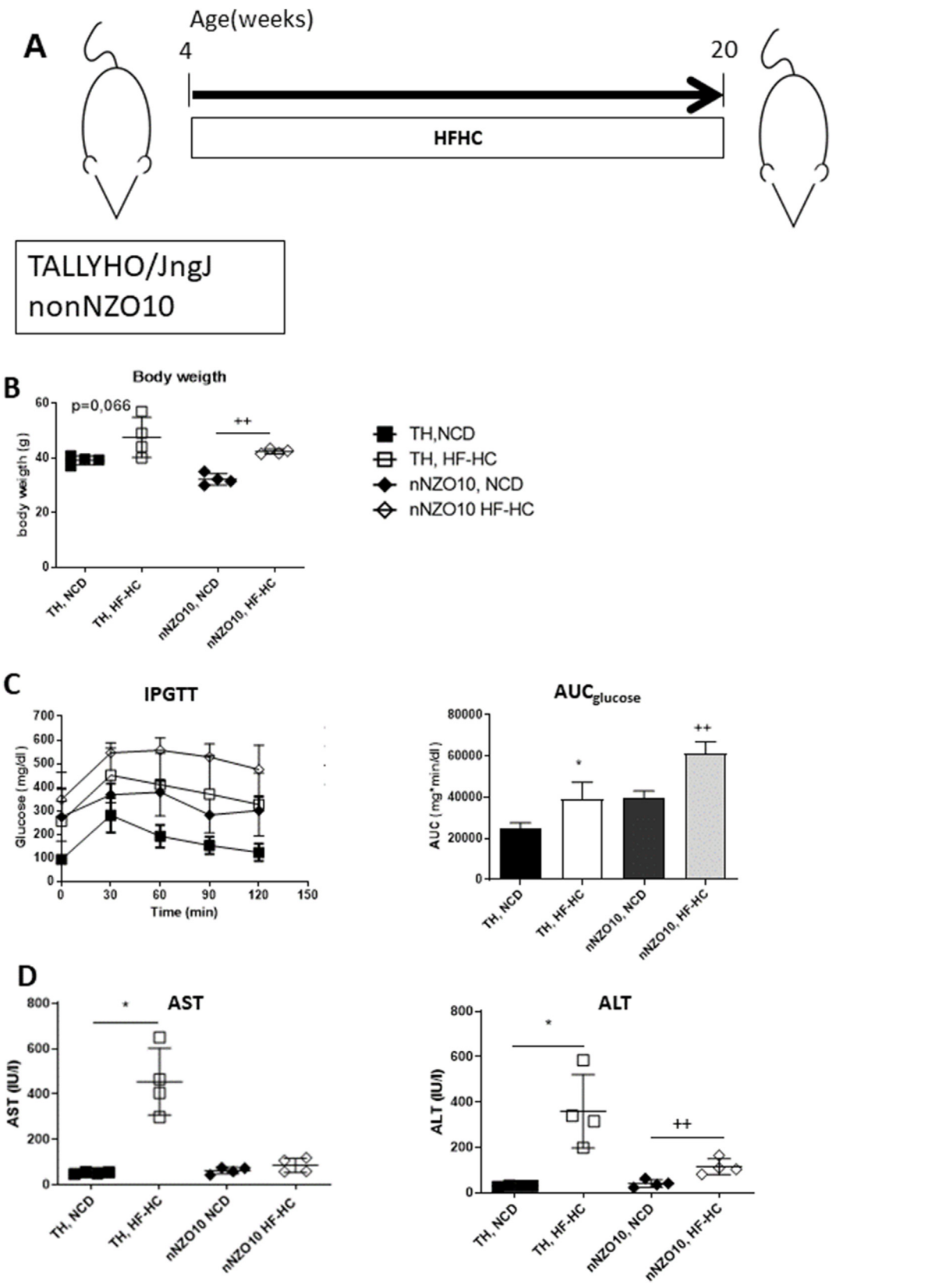

Figure 1: Onset of the metabolic syndrome after HFHC diet. (A) TALLYHO/JngJ and nonNZO10 mice were fed with HF-HC diet for 16 weeks. (B) Body weight after 16 weeks of HFHC-diet compared to NCD and weight gain over the time during HFHC diet compared to NC diet. (C) After 16weeks of HFHC diet, i.p. glucosetoleranz test was performed in all animals after 16h of fasting. (D) Biochemical analyses of alanine (ALT) and aspartate (AST) transaminases in blood serum. Data are presented as mean ± SD. Unpaired students t-test with Welsh-correction if necessary was used for comparison between treatment and control group. $n = 4$/each group. $^{*}P < 0.05$; $^{**}P < 0.01$; $^{***}P < 0.001$ was used for comparison of TH, NCD vs TH, HF-HC, $+P < 0.05$; $++P < 0.01$; $+++P < 0.001$ was used for comparison of nNZO10, NCD vs nNZO10, HF-HC.

showed elevated ALT levels after HF-HC diet (Figure 1D).The deRitis Quotient in nNZO mice was <1, whereas in TH mice, the deRitis Quotient was >1. Thus, all mice developed a persistent hepatitis after HF-HC diet, but to different degrees.

3.3. Histological development of steatohepatitis after HF-HC diet

Although elevated transaminases are important markers of inflamed liver tissue, the histological qualification remains the gold standard for the diagnosis of MASLD and MASH. All animals developed significant signs of steatohepatitis after HF-HC diet with an elevated NAS (TH, NCD: NAS 1,0 vs. TH, HF-HC, NAS: 5.5; $p = 0{,}0013$) (nNZO10, NCD: NAS:0 vs. nNZO10, HF-HC NAS: 3, $p < 0{,}0005$) (Figure 2A+B). Histological MASH was most pronounced in TH, particularly with increased steatosis and ballooning (Supplementary Table 1). Severe liver steatosis was also reflected by elevated liver weight and increased intrahepatic liver triglyceride content in both strains (Supplementary Figure 1D). Importantly, both strains developed significant liver fibrosis compared to controls (Figure 2 C,D+Supplementary Figure S1 E). Histological features in human MASH include macrovesicular steatosis, lobular inflammation and ballooning degeneration of hepatocytes, which are reflected in the NAS score [27]. Compared to human samples, TH mice showed in particular similar degree of hepatocyte ballooning and steatosis (Figure 2A+2E).

3.4. Activation of innate and adaptive immune systems in the progress to MASH

While the importance of the innate immune system in the contribution to liver inflammation is widely accepted, less is known about the role of the adaptive immune system in relation to progression. Therefore, we analyzed the intrahepatic immune system using flow cytometry. We found significant increase in the absolute numbers of intrahepatic B cells, T cells and in detail of $CD4^+$ and $CD8^+$ T cells in TH mice after HF-HC diet (Figure 3A). We could also show a many-fold increase of $CD4^+Foxp3^+$ regulatory T cells (Tregs) after HF-HC diet (Figure 3A).
After MASH induction in nNZO10 mice, there was a marked shift of intrahepatic cells towards more B cells. Within the T cell population, we could show a proportional decrease in $CD4^+$ T cells with a consequently increase of $CD8^+$ T cells (Supplementary Figure S2 A).
The subset of liver macrophages includes resident Kupffer cells (KC) with $CD11b^{neg/low}$ and $F4/80^{high}$ expression, which are resident phagocytes as well as monocyte-derived macrophages (MoMF), characterized by $CD11b^{high}$ and $F4/80^{high}$ expression. MoMFs could be further subdivided into $Ly6C^{high}$, which are associated with a proinflammatory phenotype [28,29].
As nNZO10 mice showed only mild histological inflammation, we did not detect significant changes in the macrophages subsets. Consistent with histological evidence of inflammation, MoMFs were significantly increased in TH after HF-HC diet (Figure 3B), particularly with increased levels of $Ly6C^{high}$macrophages. Intrahepatic dendritic cells ($CD11c^+$) were also increased.
In conclusion, activation of both the innate and adaptive immune systems are important pathways contributing to MASLD, particularly in TH mice.

3.5. Development of MASH is characterized by increased inflammation, oxidative stress and ER stress as well as disrupted lipid metabolism and followed by activation of profibrotic pathways

In order to detect the early disease changes and analyse pathophysiological pathways, we analyzed several gene expressions in the liver, representing key transcripts in the pathways of inflammation, fibrosis and fatty acid metabolism.
Consistent with hepatic steatosis and dyslipidemia, mRNA expressions of *FGF21* and *CD36* were significantly upregulated after HF-HC-diet in both groups (Figure 4A). The Sterol regulator element binding proteins (*SREBPs*), a family of transcription factors involved in the lipid biogenesis, were significant downregulated. Furthermore, the expressions of pro-fibrotic markers *Col1a1 and TIMP1* were also upregulated after 16 weeks of HF-HC diet, mostly in TH mice (Figure 4B).Consistent with histological inflammation, proinflammatory molecules such as *CCL2*, *NOS2* and *TNF-alpha* were highly transcribed in TH mice (Figure 4C). Due to small numbers of nNZO mice, the result of Nos2 may not be valid for this gene. As oxidative stress and ER-stress are crucial factors in the development of steatohepatitis, we measured the expression of the most important antioxidant genes. We could show a significant downregulation of *Catalase* and a tendency to decrease *SOD* after HF-HC diet in TH mice. (Figure 4D). In conclusion, we could show that 16 weeks of HF-HC diet induced the development of MASH also at the molecular levels, represented by increased inflammation, fibrosis, and disturbed lipid metabolism.

3.6. Mass-spectrometry based hepatic proteomics demonstrated enrichments of proteins related to the lipid metabolism

We further analyzed the changes in the liver proteome after HF-HC diet. A total of 4536 proteins were discovered with a false discovery rate of <1% in the TH group. After quantification, a total of 872 proteins found to be significantly differentially expressed between HF-HC and NCD (absolute log2 fold change >0.5, *q*-value <0.05).
Using overrepresentation analysis (ORA) we further classified the differentially expressed proteins into the different KEGG pathways [30]. Here, we could show that the most highly enriched proteins were associated with pathways belonging to the lipid metabolism and PPAR signaling (e.g. *Fabp4* and *PLIN2*) as well as with glucose metabolism (e.g. *pkm*), complement and coagulation cascades in TH mice (Figure 5A). Proteins involved in the steroid biosynthesis pathways, linoleic acid and metabolism pathways are downregulated.
In nNZO mice, we detected a total of 4536 proteins with a false discovery rate of <1%. A total of 531 proteins were significantly differentially regulated. Overrepresentation analysis revealed that most of the significantly upregulated proteins were associated with KEGG pathways of protein digestion and absorption, peroxisome and lipid metabolism, and extracellular matrix interaction. Proteins associated with steroid biosynthesis and linoleic acid metabolism were downregulated (Figure 5B).
In conclusion, these results emphasize the metabolic dysregulation as well as the pro-inflammatory status in both models.

3.7. Transcriptomic profile of humans with MASH and severe obesity

To confirm the translational nature of our mouse models, we the compared transcriptomic profile of humans with MASH and severe obesity to our mice models. We analyzed the differentially expressed genes between patients with obesity and MASH compared to patients with obesity, but without any hepatic steatosis, comparable to our mouse models. Here, we could show distinct transcriptomic profile (Figure 4E,F). Further gene ontology™ evaluation revealed a major upregulation of genes involved of proinflammatory pathways such as leukocyte chemotaxis and adhesion, immune response activating signaling and neutrophil chemotaxis. In detail, we could show similar upregulation of *TNF* and *CCL2* compared to TH and nNZO.
On the other hand, several genes involved in metabolic processes are downregulated. In particular, pathways belonging to the response to

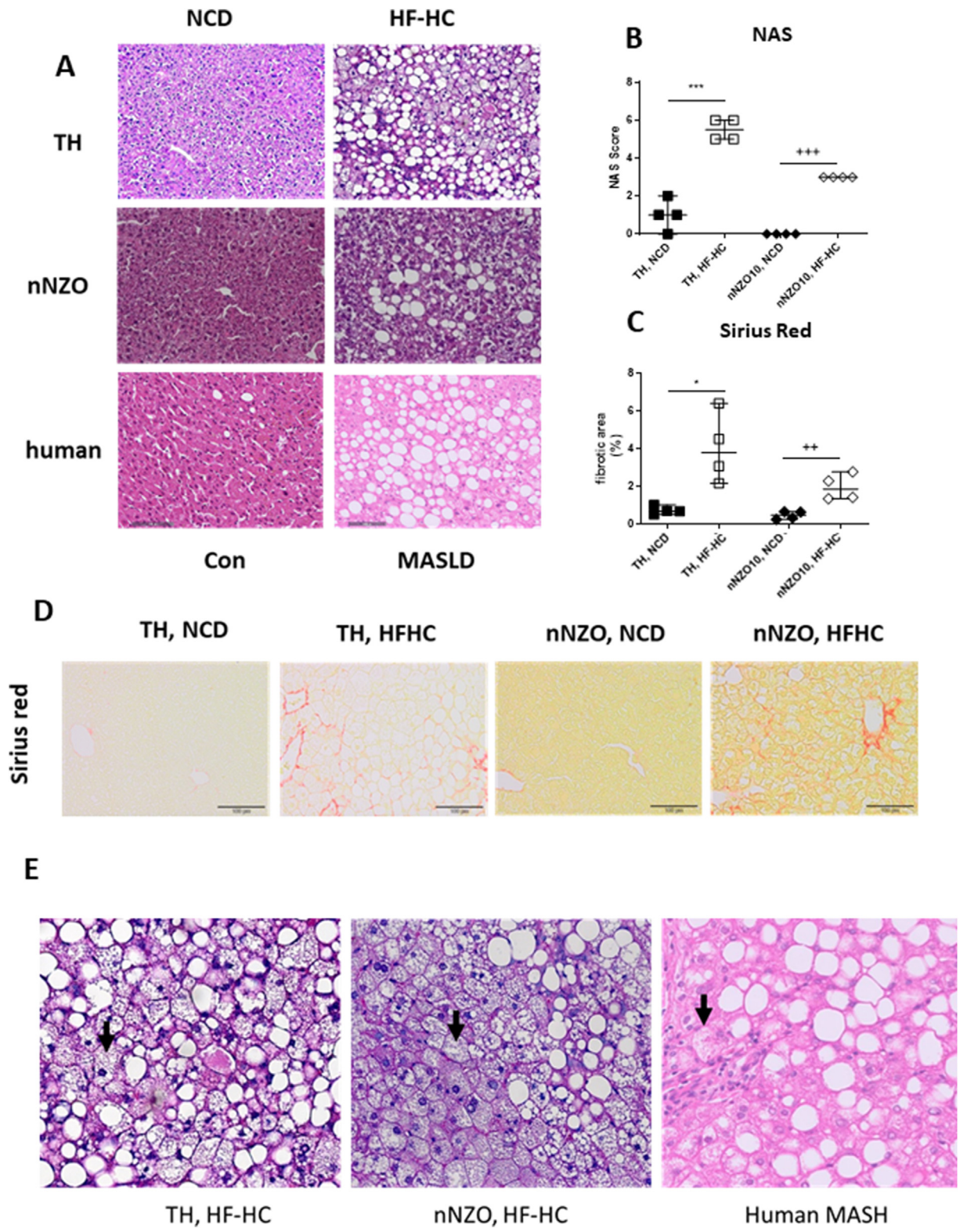

Figure 2: Histological development of MASLD. (A) Representative images of liver sections stained with haematoxylin and eosin (H&E) for assessment of liver histology and with periodic-acid Schiff reaction (PAS) for assessment of glycogen accumulation and with Sirius red for evaluation of fibrosis (magnification $\times 20$) for each group prove development of NASH. (B) Histological grading of NASH using the NAFLD-activity score (NAS). Data are presented as median with IQR. Non-parametric Mann—Whitney test was used for comparing two groups. (C) Percentage of fibrosis was assessed by analyzing four microscopic fields at $\times$ 100 magnification and showed significant increased fibrosis after HFHC diet in both strains. (D) Sirius red staining. (F) Hepatic ballooning in TH and nNZO, indicated by black arrow, is comparable with human MASH. Data are presented as mean $\pm$ SD. Unpaired t-test with Welsh-correction if necessary was used for comparison between of two groups. $n = 4$/each group. $^{*}P < 0.05$; $^{**}P < 0.01$; $^{***}P < 0.001$ was used for comparison of TH, NC D vs TH, HF-HC. $+P < 0.05$; $++P < 0.01$; $+++P < 0.001$ was used for comparison of nNZO10, NCD vs nNZO10, HF-HC.

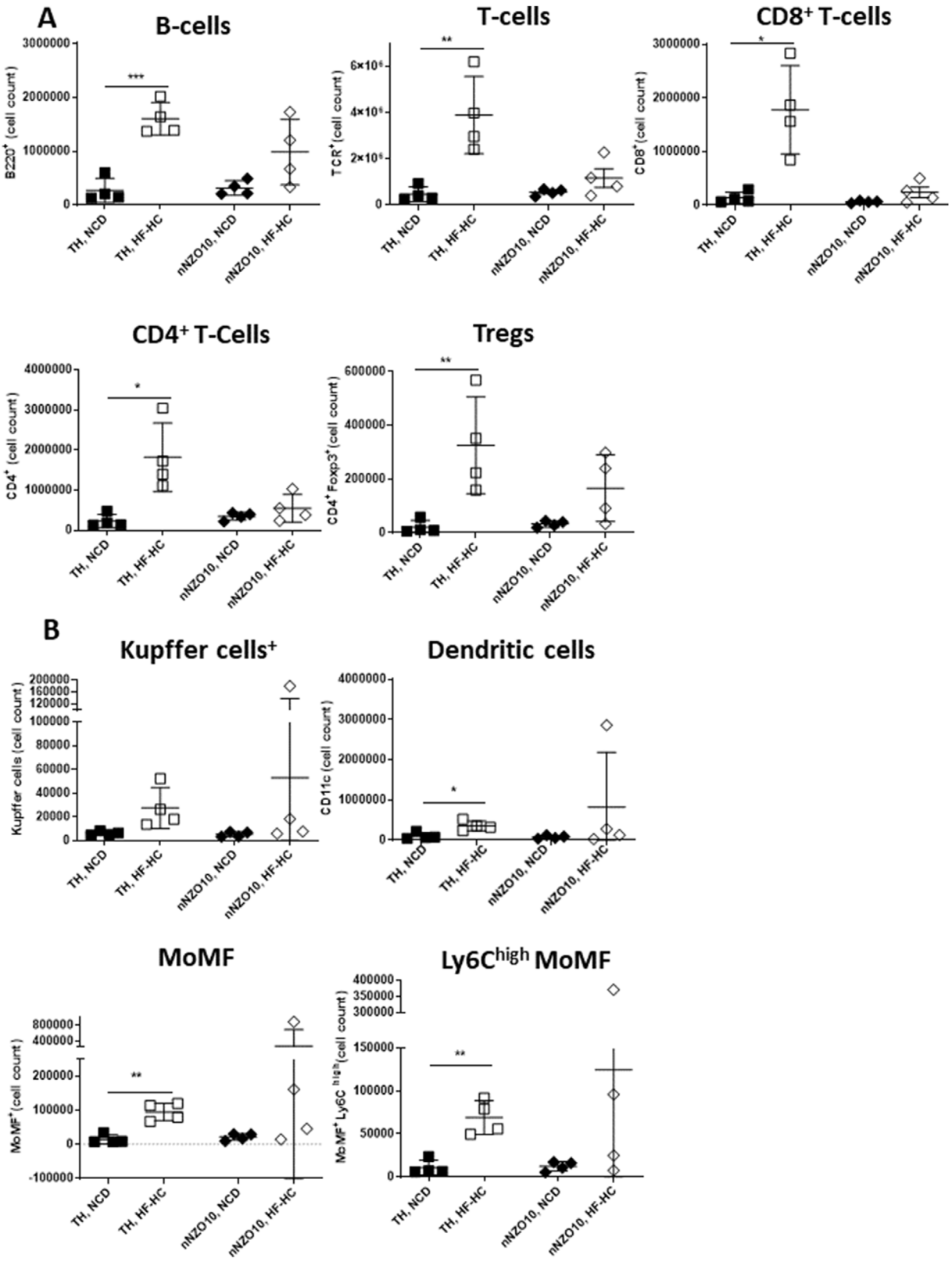

Figure 3: Flow cytometry analyses of the innate and adaptive immune system. (A) Flow cytometry analyses of the adaptive immune system focusing on the intrahepatic subsets of CD4+ T cells and CD8+ T cells (B) and subsets of intrahepatic liver macrophages and dendritic cells. Data are presented as mean ± SD. Unpaired students t-test with Welsh-correction if necessary was used for comparison between treatment and control group. $n = 4$/each group. $^{*}P < 0.05$; $^{**}P < 0.01$; $^{***}P < 0.001$ was used for comparison of TH, NCD vs TH, HF-HC. $+P < 0.05$; $++P < 0.01$; $+++P < 0.001$ was used for comparison of nNZO10, NCD vs nNZO10, HF-HC.

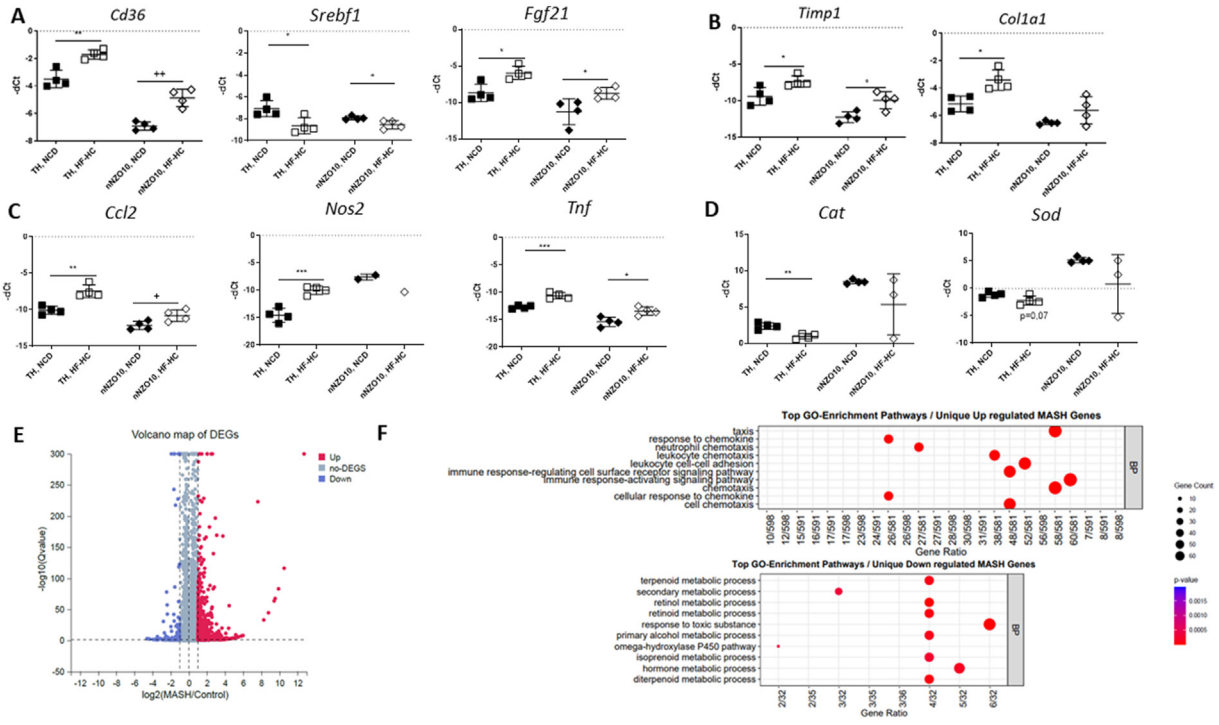

Figure 4: Gene expression representing pathways of inflammation, ER-stress, oxidative stress, lipid metabolism and fibrosis is comparable to human transcriptomic profile. After analyzing gene expression with the Fluidigm Real-Time PCR Analysis Software, genes that were expressed significantly different upon PCA were exemplarily chosen to visualize changes in the pathways of inflammation (A) lipid metabolism (B) fibrosis (C) inflammation (D) oxidative and ER-stress. (E) Volcano plot of differential expressed genes form human transcriptomics analyses. (F) Gene ontology™ classification of DEG. $n = 4$/each group*. *NOS2: nNZO10, NCD: $n = 2$; nNZO10, HF-HC: $n = 1$. *Cat: nNZO10, HF-HC: $n = 3$. *SOD: nNZO10, HF-HC: $n = 3$. *$P < 0.05$; **$P < 0.01$; ***$P < 0.001$ was used for comparison of TH, NCD vs TH, HF-HC. +$P < 0.05$; ++$P < 0.01$; +++$P < 0.001$ was used for comparison of nNZO10, NCD vs nNZO10, HF-HC.

toxic processes, including ER-stress are downregulated, which is comparable to downregulation of murine *catalase* and *SOD*.

In conclusion, the transcriptomic profile of patients with MASH and severe obesity reveals a significant upregulation of proinflammatory processes, which is in line with the activated proinflammatory immune response and the upregulation of proinflammatory genes in TH and nNZO mice.

3.8. Development of MASLD after HF-HC diet is associated with changes in the microbiota

When analyzing the composition of the microbiota, we could detect a decreased alpha-diversity after HF-HC diet as well as changes in beta-diversity in nNZO10 mice, which is highlighted by the distinct proximate distance between HF-HC and NCD mice in nonmetric multidimensional scaling (MDS) (Figure 6A—C). TH also developed significant changes int beta-diversity with a shift towards both *Actinobacteria* as well as *Proteobacteria* (Figure 6B).

Thus, we were able to show for both strains that development of metabolic changes and MASLD are further associated with changes in microbiota.

3.9. TALLYHO/JngJ mice develop signs of kidney injury after HF-HC diet

After 16 weeks of HF-HC diet, we evaluated the kidney function of TH mice. Here, increased expression of Neutrophil Gelatinase Associated Lipocalin (NGAL) was detected, which is a valuable marker for early detection of renal injury [31] and kidney injury molecule-1 (KIM-1) was increased [32]. In addition, a decreased mRNA expression (Figure 7A) of the endothelial cell marker CD31 was detectable. The protein expression pattern was additional evaluated by confocal immunofluorescence imaging (Figure 7C). To determine the origin of renal injury, mRNA detection of pro-inflammatory pathways was performed, which showed an increase in IL-6, C3, and IL-1β expression compared to the NCD group (Figure 7B). Confocal immunofluorescence imaging of paraffin-embedded kidney sections showed no generalizable difference for protein expression of nephrin, and fibronectin between the groups (Supplementary Figures 3B-D).

Thus, TH mice developed signs of acute kidney injury after 16 weeks of HF-HC diet, which might then lead to chronic kidney injury in the long term. Therefore, we validated the TH mouse model as the most encouraging one.

3.10. SGLT2-inhibitor empagliflozin improves histological outcome of MASLD and reveals anti-inflammatory potentials

Recently, large trials have shown beneficial effects on diabetic MASLD in patients without overweight [17,18,33], but the effect in patients with obesity is still in debate. Therefore, we tested SGLT2i empagliflozin in our TH mouse model.

In the obese TH mouse model of MASLD, empagliflozin significantly improved hyperglycemia, but had no effect on body weight (Figure 8 A) or amount of adipose tissue after 4 weeks of treatment (Supplementary Figure S4). Interestingly, empagliflozin significantly reduced the intrahepatic amount of triglyceride and also reduced the liver weight (Supplementary Figure S4 A).

Most important, we could demonstrate a significantly attenuated histological onset of MASLD after empagliflozin treatment (Figure 8 B), in particular with histological improved liver steatosis (Supplementary Table 3). Alongside with histological improvement of steatohepatitis,

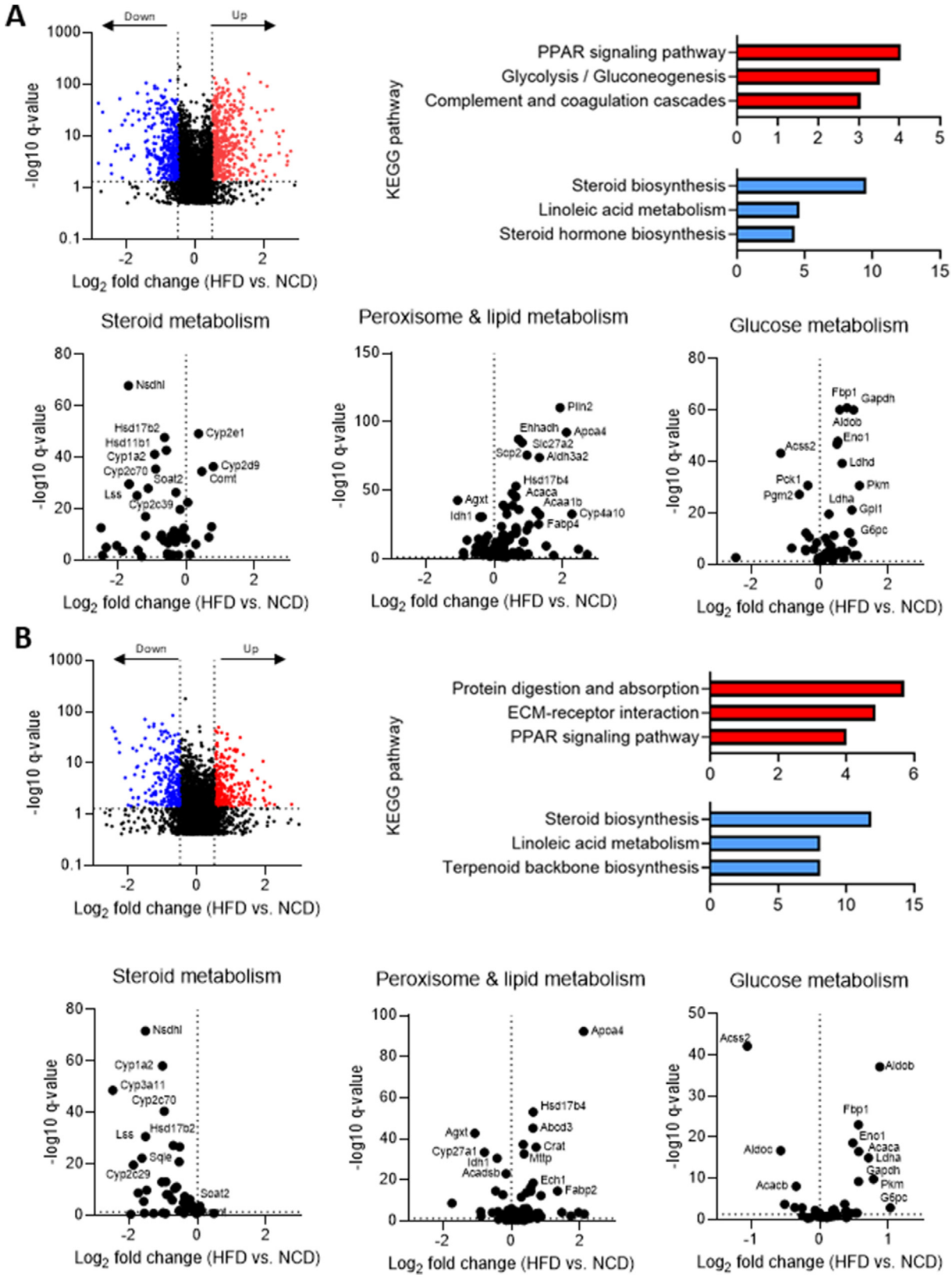

Figure 5: Mass spectrometry based liver proteome analysis. Liver proteomic analysis in TH NCD vs TH, HF-HC (A) and in nNZO NCD, vs nNZO, HF-HC mice (B). Vulcano-plot of log2 fold changes of individual proteins in liver samples of NCD vs. HF-HC. Proteins with an absolute log2 fold change of >0.5 and q-value of 0.05 are highlighted in blue (down-regulated) and red (up-regulated). Overrepresentation analysis (ORA) of KEGG pathways among significantly up-regulated (red) and down-regulated (blue) proteins (q-value <0.05, absolute log2 fold change >0.5) in livers of HF-HC fed mice vs. NCD. Vulcano plots of log2 fold changes of proteins annotated to pathways of Peroxisome & lipid metabolism, Glucose metabolism and Steroid metabolism. $n = 4$ for all comparisons.

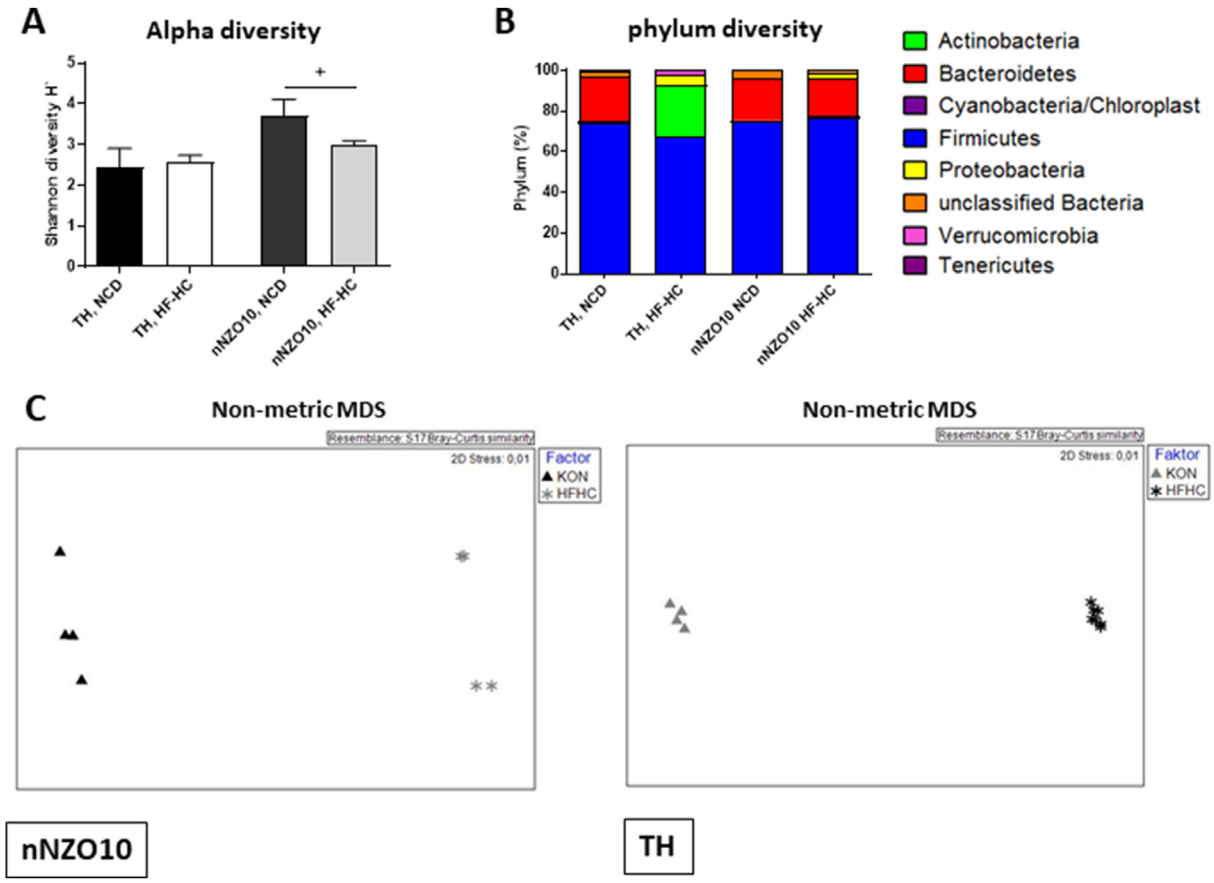

Figure 6: Changes in the microbiota after HFHC diet and onset of MASLD. (A) Analyzing the alpha diversity after 16 weeks of HFHC diet (B) Illustration of microbiome composition of phyla after 16 weeks of HF-HC diet. (C) Non-metric MDS plot for illustration of beta-diversity after 16 weeks of HFHD diet. $n = 4$/each group.

we could demonstrate a histological improvement of hepatic fibrosis (Figure 8B). Interestingly, we could not detect a significant reduction in AST and ALT levels (Supplementary Figure S4).

Analyzing the intrahepatic immune cells, treatment with empagliflozin significantly reduced the absolute numbers of intrahepatic B cells, T Cells and their subsets of $CD8^+$ and $CD4^+$ T cells as well as Tregs (Supplementary Figure S5). This decrease was also visible in the percentage amount of intrahepatic immune cells.

These histological and cellular improvements of inflammation and hepatic steatosis were also detectable on transcriptomic level (Figure 8C). In line with histological improvement, we could show reduced levels of *fgf21* and reduced levels of pro-fibrotic genes, such as *col1a1* and *timp1*. Furthermore, pro-inflammatory genes, such as *NOS2*, *CCl* and *TNF* were downregulated after treatment with empagliflozin. Additional, the major player of anti-oxidative defense, *catalase (CAT)* and *superoxide-dismutase (SOD)* were significantly upregulated in empagliflozin-treated mice.

In summary, we could demonstrate that empagliflozin treatment improves histological onset of MASLD by reducing hepatic steatosis even without weight loss in the TH-mouse model of diet-induced steatohepatitis. Empagliflozin further reveals anti-inflammatory potential and improves anti-oxidative defense.

4. DISCUSSION

Although the human pathogenesis of MASLD could not be simulated in every detail, animal models are of great importance both for further understanding of distinct mechanism and for preclinical testing of pharmacological treatments. Since the new definition of MASLD, mouse models should display not only the clinical and histological onset of steatohepatitis, but also the presence of cardiometabolic risk factors such as obesity, insulin resistance or dyslipidemia [34,35]. Ideally, a preclinical mouse model of MASLD should share same characteristics as the human disease related to the cause of disease, clinical phenotype, histological disease manifestations and gene expression. An important risk factor for the development of MASLD is central obesity [36], which can be induced by overnutrition, sedentary lifestyle and genetic predisposition. While both strains have already the genetic predisposition for obesity under NCD [9,37], TH and nNZO develop even more pronounced obesity after 16 weeks of HF-HC, which is comparable to common monogenetic mouse models for obesity such as leptin deficient *ob/ob* or *db/db* [8] and also to the DIAMOND mice model of MASH [38]. However, *ob/ob* mice develop steatohepatitis only with an additional stimulus and appear to be protected from developing fibrosis even with an additional MCD diet [39]. Furthermore, lipotoxicity is an important driver in the progression from simple steatosis to steatohepatitis [40]. In MASLD, hepatic accumulation of FFA is associated with upregulation of various proteins involved in the lipid metabolism, which is also present in our models, such as upregulation of *apolipoprotein-a-IV (apoa4)*, which may reflect adapting response to lipid overload [41]. On the other hand, upregulation of *fatty acid binding protein (fabp4)* and *fatty acid transport protein 2 (fatpP2/scl27A2)* was found in both models. *Fabp4* is a key player in the pathophysiology of liver steatosis as it is involved in FA

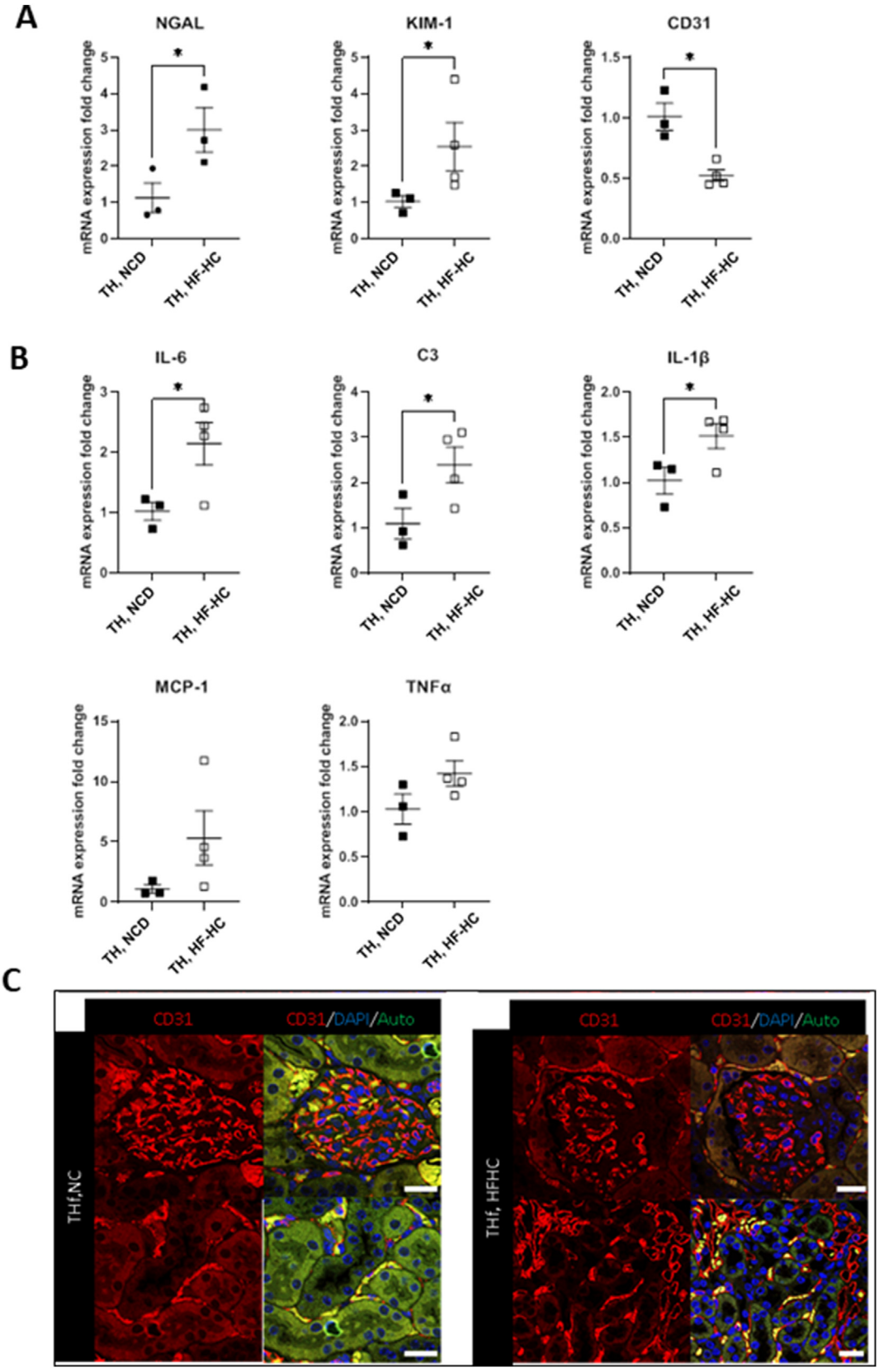

Figure 7: Development of acute kidney injury after HF-HC diet in TH mice. (A) Normalized mRNA expression (qPCR) in the murine kidneys of markers for kindney injury and (B) and proinflammatory markers in TH, NCD compared TH, HF-HC (TH, NCD $n = 3$; TH, HF-HC $n = 4$). Unpaired t test with Welch's correction ± SEM was used for the comparison of TH, NCD, and TH, HFDHC groups. (C) Immunofluorescence staining for CD31.

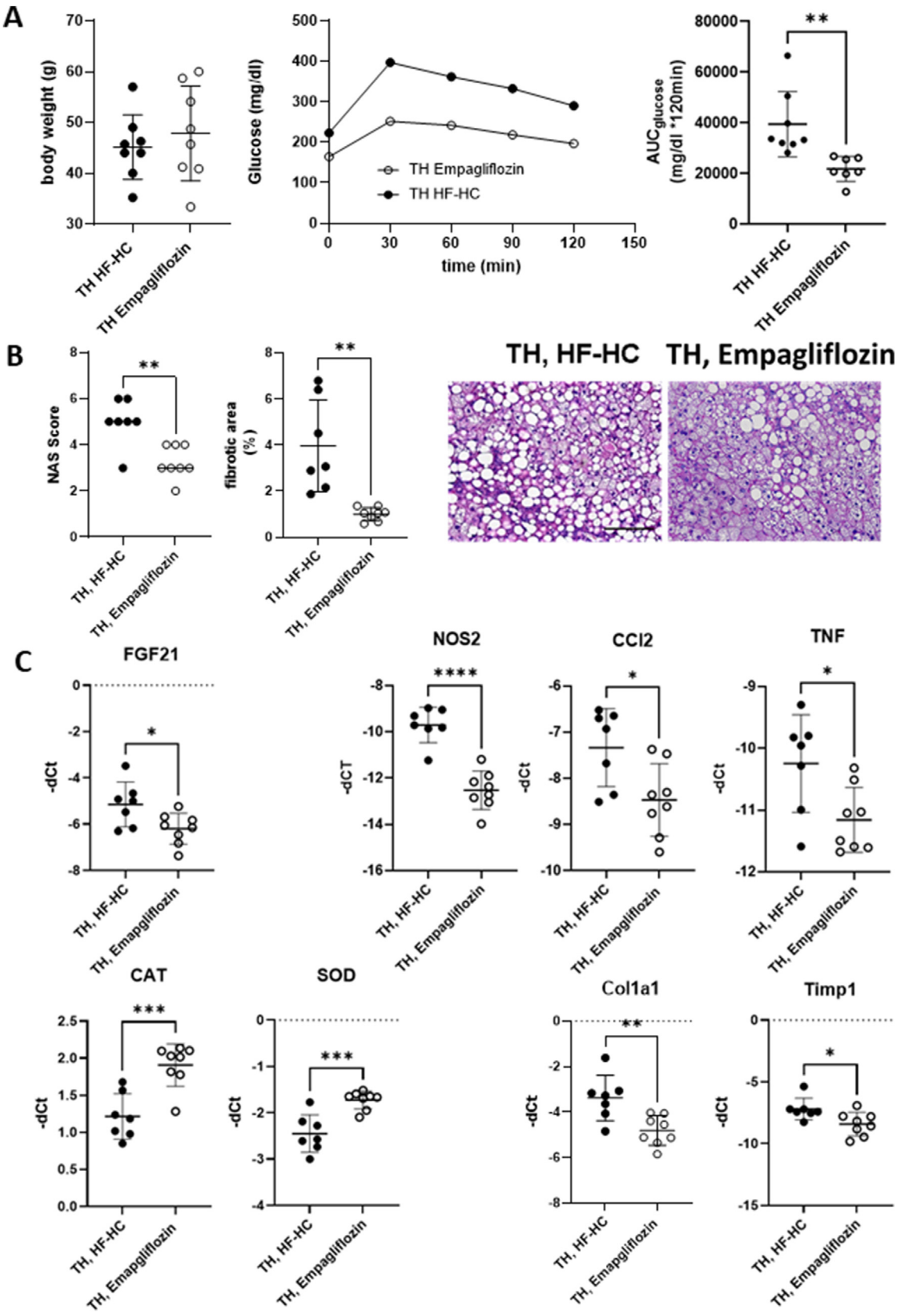

Figure 8: Empagliflozin improves diet-induced steatohepatitis in TH mice. (A) Empagliflozin improves hyperglycemia, but does not effect obesity. (B) Treatment with empagliflozin significantly improves histological onset of steatohepatitis and fibrosis. (C) Impact of empagliflozin on pathways of lipid metabolism, inflammation oxidative stress and fibrosis. Data are presented as mean ± SD. Unpaired students t-test with Welsh-correction if necessary was used for comparison between treatment and control group. $^{*}P < 0.05$; $^{**}P < 0.01$; $^{***}P < 0.001$ was used for comparison of TH, HF-HC vs. TH, empagliflozine.

uptake, but could also promote inflammatory response due to ER stress and oxidative damage [42,43]. Increased intrahepatic *fabp4* expression is considered as a predictive biomarker for disease progression in MASLD and associated with a poor prognosis. In addition, increased expression of *scla7a2* and its receptor *CD36* are known to be associated with fatty liver disease as overexpression contributes to enhanced influx of free fatty acids and correlates with disease progression [44–46]. Furthermore, upregulation of *plin2 (Perilipin 2*), which regulates the triglyceride storage and mobilization, is associated with increased lipid accumulation in hepatocytes [47,48]. In addition, it could induce pro-inflammatory pathways and thus promote the development of fibrosis. Therefore, these proteomic changes may be indicative of an already disturbed lipid metabolism, particularly in TH. Additional, human studies have shown downregulation of *SREBF-1* in end-stage MASH and advanced fibrosis [49], which was also detectable in both mouse models and may indicate a depleted lipid metabolism. In addition, we noticed upregulation of enzymes and proteins, associated with the peroxisome pathways and beta-oxidation, such as acaca or cyp4a10 [50,51] and promote oxidative stress in the long term. Furthermore, the downregulation of alanine glyoxylate aminotransferase (AGXT) and lactate dehydrogenase 1 (LDH1) leads to impaired lipid detoxification processes, increased oxidative stress and dysregulated lipid metabolism, contributing to the development of steatohepatitis. Koliaki et al. demonstrated that hepatic catalase activity was significantly decreased in humans with MASH [52], antioxidant defenses and being associated with end-stage MASH [53]. In addition, *Hspa5* was significantly downregulated in our mice models, reflecting increased ER stress and is also associated with disease progression [54]. Taken together, these data suggest an impaired lipid metabolism and lipid detoxification processes, particularly in TH mice, which may then contribute to the development of steatohepatitis, as oxidative stress due to lipotoxicity is known to be an important trigger in driving the immune response in MASLD [55]. A recent study also demonstrated significant alteration in lipid metabolism, particularly for fatty acids and triglycerides in a CCL4-induces MASH model, which was comparable to human alterations in MASH [56]. Therefore, our data also may indicate a good metabolic resemblance to human MASH. Histologically, both strains in our models develop the onset of steatohepatitis and therefore fulfil the necessary criteria for a murine model of MASH [57]. In particular, the extent of hepatocyte ballooning as the histological key feature of human MASH [58] is comparable to human disease manifestation. Although they only develop mild histological signs of inflammation, we were able to demonstrate the significantly increased accumulation of proinflammatory cells in the liver by flow cytometry. In addition, liver injury in both models is expressed by elevated transaminases. In line with the histological findings, transaminase elevation was more pronounced in TH and comparable to other established suitable mice models. Also, de Ritis Quotient >1 may also indicate severe disease hepatocyte damage in this model. The presence of fibrosis is not necessary for the diagnosis [27]. Mice developed mild fibrosis in both models, which is consistent with recent findings from large cohorts of patients with severe obesity [59], where the majority of patients had only mild fibrosis [60]. In addition to increased fibrotic areas on histology, we also showed a significant increase of *Col1a1* and *TIMP-1* and hydroxyproline levels, which are associated with fibrosis [61].

The onset of human steatohepatitis is characterized by infiltration of B- and T cells [55], particularly $CD4^+$ and $CD8^+$ T cells. $CD4^+$ cytokine production is then a potent stimulus for activation of pro-inflammatory macrophages, which are important drivers of chronic inflammation and fibrosis [62]. The significant increase in T_{regs} may reflect an imbalance between pro-inflammatory and regulatory T cells, which is associated with progression from simple steatosis to MASH [63] and is also a risk factor for the development of hepatocellular carcinoma [64]. Interestingly, nNZO10 mice showed a percentage shift with a decrease in T cells and $CD4^+$ T cells. *Ma* et al. [65] previously reported about a loss of $CD4^+$ T cells during of the development of steatohepatitis, which then promotes hepatocarcinogenesis.

Furthermore, CD8+ T cells seems to play an important role in immune-mediated immune-mediated metabolic diseases such as MASH [66]. Comparable to the human disease, we detected a significant increase of CD8+T Cells in TH mice along with a significant increase of *Tnf*. Interestingly, portal infiltration of CD8+ T Cells is associated with disease severity [67] in humans.

Macrophages also play a key role in the pathogenesis of steatohepatitis and the onset of inflammation. In particular, the recruitment of monocyte-derived macrophages has been associated in humans with steatohepatitis and onset of fibrosis [62]. Analogue to the human phenotype, we could demonstrate infiltration of bone marrow-derived pro-inflammatory Ly6C + monocytes in TH mice.

There is recent evidence that B cells are also involved in the disease progression. It has been shown that B cells accumulate in the liver and promote further fibrosis and inflammation by increased secretion of TNFα and IL-6 [68]. In line with these previous findings and the signature of intrahepatic immune cells in both mouse models, we could also demonstrate in our human samples a significant upregulation of transcriptomic pathways, which are related to cellular immune response, such as leucocyte chemotaxis, immune-response-activating signaling pathways or immune response-regulating cell surface receptor signaling pathways.

In summary, these results elucidate the important role of adaptive and innate immune cells in the distinct pathogenesis of MASLD. Comparing both mice models, the onset of MASLD was more pronounced in TH mouse model, while the nNZO mouse model could be rather classified as an early stage of MASLD. Therefore, these data manifest the important role of the cellular inflammation in the progress from simple steatosis to severe steatohepatitis.

The microbiome composition differs in different diseases and microbiota changes have also been described for MASLD [69]. Important features are alpha- and beta-diversity. Alpha diversity represents the distribution of species abundances in a given sample and is indicated-among others-by the Shannon score. Beta diversity describes the similarities between different samples [70]. Although there are differences between changes in animal studies and human studies, the heterogeneity of different genera and the ration of the most dominant phyla of bacteria *Firmicutes* and *Bacteriodetes* are important [71]. In both mouse models, we could show a significant reduced beta diversity, while nNZO10 mice also developed a significantly reduced alpha diversity after HF-HC (Figure 6A). A recent study by the group of *Loomba* et al. showed an association between increased abundance of *Proteobacteria* and decreased abundance of *Firmicutes* in patients with moderate to severe fibrosis [72] as we could show in TH mice. The increase abundance of *Actinobacteria* is also remarkable in TH mice and in line with a previous study in pediatric patients with MASLD [73]. Although the changes in the microbiome are consistent with the overall picture of MASLD in both strains, one should be aware that the diet itself has a strong influence on the stool microbiome [74] and may also contribute in part to the changes in microbiota composition.

In conclusion, both mice models represent the main features of the human pathogenesis of steatohepatitis in addition to the presence of cardiometabolic risk factors as postulated recently [35,57,75] and illustrate the important molecular changes in the development of

MASLD comparable to the human disease. Comparing both models, we validated the TH as the most encouraging mouse model for MASLD as the onset of MASLD and its distinct changes are more pronounced and may better resemble the full picture of human MASLD. Furthermore, the majority of commonly used mouse models use male mice, so female mice models are rare in this field, but urgently needed compared to the large proportion of female participants in the human MASLD trials. Although it has been previously described that female mice seems to be less vulnerable to HFD-induced MASLD [76], we were able to show that our female TH mice model showed even more pronounced disease activity compared to male nNZO mice. In particular, TH mice developed increased intrahepatic T cell accumulation and activation, although a previous study described sex-dependent T-cell dysregulation [77].

We therefore hope that our mouse model could serve as an additional platforms for further mechanistic and therapeutic studies in MASLD, in addition to the already existing mouse models.

It is already known that patients with MASLD have a higher prevalence of kidney disease and the severity of kidney disease also appears to be also associated with the severity of MASLD [78]. In addition, renal failure is strongly associated with increased mortality in patients with liver cirrhosis [79]. Recently, the group of *Sun D.Q* et al. showed, that using the proposed definition of metabolic-associated fatty liver disease (MAFLD), the association between patients with MAFLD and chronic kidney disease is even stronger [80], highlighting the need for animal models that reflect this coexisting disease. Previous have shown that high-fat diets can induce diabetic kidney disease as a result of a high-fat diet [81]. Consistent with these findings, we were able to demonstrate the onset of kidney injury, characterized by increased expression of KIM1 and NGAL as established markers for kidney injury [82]. The identified increase inIL-6, which has been associated with changes of the glomerular endothelial cell permeability and mesangial cell proliferation [83], supports the presence of a renal inflammatory state. The increase in C3 expression may imply activation of the complement system which has been previously demonstrated in diabetes models [84]. Furthermore, the release of IL-1β is a key component of the sterile inflammation that has been shown to induce both onset and progression of diabetic kidney disease, whereas inhibition of IL-1β function preserves renal morphology and the glomerular filtration rate (GFR) in db/db mice [85]. Previous studies have been shown that increased expression of MCP-1 directly correlates with interstitial cellular infiltration and the degree of albuminuria [86], both important factors of kidney injury. Surprisingly, there was no change in Fibronectin as an indicator for fibrosis detected. However, as we were able to demonstrate features of kidney injury, fibrosis might develop after prolonged feeding period. Overall, the TALLYHO/JngJ high fat high carbohydrate model might represent an early phenotype of kidney dysfunction, which is mainly driven by proinflammatory pathways. Nevertheless, further investigations would be beneficial to completely picture the phenotype of kidney disease.

With regard to the new definition of MASLD, mouse models must to display both the features of the metabolic syndrome such as obesity, insulin resistance and dyslipidemia and the clinical and histological onset of steatohepatitis [34,35]. Just recently, with the aim to harmonize the terminology for pre-clinical mouse models, the concept of "Diet-induced steatohepatitis" with naming the additional clinical features was discussed [35]. There is already a huge landscape of mouse models, with dietary mice model being the most common followed by genetic modified mice. However, only very few mouse models could satisfy most of the criteria for an "ideal" mouse model so far [87]. Although genetic models-mostly based on single gene alternations such as *ob/ob* may be convenient for certain studies, they do not reflect the polygenetic background in human MASH and do not adequately reflect the human pathogenesis [87,88]. In terms of diet, Teufel et al. demonstrated that fructose-enriched murine model showed the greatest similarity with the human pathogenesis of MASH compared to other diet-induced models [39]. This may be explained by the increased hepatic de novo lipogenesis, hepatic fat content and increased hepatic insulin resistance after fructose intake, which is confirmed for both human and mice [89,90]. The cholin-deficient diet in addition to HFD could induce a fast fibrosis induction and a severe histological phenotype, which also progressed to hepatocellular carcinoma. However, in contrast to both our models and the human phenotype, there are reduced glucose and insulin concentrations, reduced circulating cholesterol- and triglyceride concentrations and only very little weight gain observed in these models [90]. Therefore, the CDAA-HFD model does not represent the features of the metabolic syndrome and could represent the new concept of MASLD only to a very limited extent. Both models in this study could nearly fulfil all requirements for an ideal mouse model of diet-induced steatohepatitis with the metabolic syndrome as they display both the main features of the metabolic syndrome and the clinical and histological phenotype of steatohepatitis [34] and are therefore at least equal to the so far most validated mice models, such as DIAMOND mouse model [38] (Supplementary Table S2), but in shorter experimental time. However, common dietary or genetic altered mouse models often struggle with the molecular differences between human and mouse and therefore could not mimic every molecular detail. In this regard, chimeric mouse models are another strategy, that could overcome the molecular differences between murine and human liver function [91]. A recent study demonstrated a similar molecular signature in humanized mouse liver after HF-HC diet compared to human MASLD [75]. In particular, metabolomics and lipidomics showed important similarities to clinical MASLD in humans. However, this mouse model did neither develop obesity nor insulin resistance as important features of the metabolic syndrome and therefore does not fulfil the recent criteria for MASLD. It also did not develop any grade of inflammation due to the immunosuppression and is therefore unlikely to develop fibrosis. Therefore, this type of mouse model might be very suitable for detailed mechanistically studies on molecular basis of the liver, but it does not fully meet the previous mentioned requirements for an ideal murine mouse model of MASLD.

To complete the validation of this mouse model, we performed a preclinical drug testing in TH mice. While it is already well known that GLP1 receptor agonists (GLP1-RA) and the selective thyroid hormone receptor beta agonist Resmetirom improve MASLD in humans and mice [92–94], the effect of SGLT2i on MASLD has been less intensively studied and their role in MASLD is still under debate. In line with a previous study showing reduction in liver fat content in patient with well-controlled diabetes and moderate obesity [16], we also demonstrated a significant reduction of liver fat content and hepatic steatosis. Interestingly, this reduction was independent of weight loss in TH mice. In humans, SGLT2i causes mild weight loss due to increased glucosuria and the calorie loss [95]. Most studies to date have concluded that the improvement in hepatic steatosis with SGLT2i appears to be mainly determined by the amount of weight loss [16,96]. However, one study also reported about a greater improvement in lipid content despite weight loss [97]. It should be noted that a previous study in a non-diabetic mouse model of steatohepatitis did not show an improvement in hepatic steatosis or inflammation after treatment with empagliflozin. On the contrary, increased activation of pro-inflammatory and pro-fibrotic pathways have been demonstrated

[98]. Therefore, the effect of empagliflozin may be influenced by the presence of insulin resistance, as SGLT2i improve hepatic and systemic insulin resistance and further reduce hepatic de novo lipogenesis [99]. We have also shown an improvement in hyperglycemia and a reduction in hepatic de novo lipogenesis in our model. Therefore, empagliflozin may improve hepatic steatosis, particularly in the setting of insulin resistance and diabetes, by improving insulin resistance.

We further demonstrated the antioxidant capacity of SGLT2i by increased antioxidant enzyme activity, such as *catalase* and *superoxide dismutase*, after treatment with empagliflozin. Previous studies have already demonstrated the antioxidant capacity of SGLT2i [100], which is also an important factor in mediating hepatocyte injury in MASLD [101]. Empagliflozin is thought to activate the AMPKα-mediated FoxO3a and Nrf2 antioxidant defense systems, thereby protecting against lipotoxicity [102]. Additional, we could prove anti-inflammatory potential of empagliflozin as another key factor in the pathogenesis of MASLD. In addition to attenuating pro-inflammatory cytokines such as TNF and CCL2, we demonstrated a significant reduction in intrahepatic CD8+ T cells. This is in line with a recent study, reporting that empagliflozin suppresses CD8+ T cell infiltration and thereby hereby ameliorates liver injury in both mice and humans [103]. In conclusion, our data suggest that the hepatoprotective effect of empagliflozin is beyond weight loss and might be mediated by improvement of hyperglycemia and reduction of hepatic de novo lipogenesis, improvement of oxidative stress and anti-inflammatory properties of empagliflozin. Therefore, empagliflozin could be an additional treatment option for MASLD, particularly in patients with diabetes. Furthermore, given the proven protection against cardiovascular events in patients with diabetes [95], SGLT2i might be an important treatment option in patients with MASLD and metabolic syndrome. Furthermore, by testing empagliflozin in TH mouse model with comparable results to previous preclinical and human studies, we could demonstrate the suitability of the new TH mouse model for preclinical drug testing.

In conclusion, this study reports on two suitable mouse model that reflect the major feature of metabolic syndrome and diet-induced steatohepatitis in addition with kidney injury. Furthermore, the comprehensive assessment of human transcriptomics in MASH provides evidence of the metabolic and pathophysiological resemblance, especially for TH mice model. A limitation of the study might be the small number of animals in each group. Additional, data variability might indicate that not all animals might respond similarly to the diet. We have already tried to reduce the variability by using the same hierarchy of litters, but it was not possible to use all animals from the same litter. Therefore, future experimental designs should take this into account and possibly increase the group size to minimize variability. However, as we already show significant changes in this small groups, these results may provide a promising baseline for further investigation in these models. Furthermore, the clinical and histological phenotype of the control group for empagliflozin testing, which was treated equally to the TH HF-HC group demonstrate a robust clinical and genetic phenotype of diet-induced steatohepatitis in a mouse model with severe obesity. Finally, we demonstrated improvement of steatohepatitis due to treatment with SGLT2i empagliflozin in the TH mice model, so that SGLT2i might be a treatment option for patients with diabetes and MASLD.

We therefore hope that both mouse models, but in particular the TH mouse model of diet-induced steatohepatitis with kidney dysfunction could serve as an additional platform for further mechanistic and therapeutic studies of MASLD in addition to the already existing mouse models.

ACKNOWLEDGEMENTS

We thank Michaela Beese and Peter Schürmann for their technical support and Martin Hapke for support in animal handling. We thank Ingmar Mederacke for technical support. We thank the Proteomics Core facility at the Leibniz Institute on Aging, Jena for Proteomic analyses.

CREDIT AUTHORSHIP CONTRIBUTION STATEMENT

Katharina L. Hupa-Breier: Writing — review & editing, Writing — original draft, Validation, Project administration, Methodology, Investigation, Funding acquisition, Formal analysis, Data curation, Conceptualization. **Heiko Schenk:** Visualization, Funding acquisition, Formal analysis, Data curation. **Alejandro Campos-Murguia:** Writing — review & editing, Visualization, Methodology, Formal analysis, Data curation, Conceptualization. **Freya Wellhöner:** Methodology, Investigation, Formal analysis. **Benjamin Heidrich:** Writing — review & editing, Methodology, Data curation. **Janine Dywicki:** Writing — review & editing, Methodology, Investigation. **Björn Hartleben:** Writing — review & editing, Investigation. **Clara Böker:** Writing — review & editing, Investigation. **Julian Mall:** Writing — review & editing, Supervision, Conceptualization. **Christoph Terkamp:** Writing — review & editing, Supervision, Project administration, Conceptualization. **Ludwig Wilkens:** Writing — review & editing, Investigation. **Friedrich Becker:** Writing — review & editing, Visualization, Formal analysis. **Karl Lenhard Rudolph:** Writing — review & editing, Methodology. **Michael Peter Manns:** Writing — review & editing, Supervision. **Young-Seon Mederacke:** Writing — review & editing, Data curation. **Silke Marhenke:** Writing — review & editing, Methodology. **Hanna Redeker:** Writing — review & editing, Investigation. **Maren Lieber:** Writing — review & editing, Investigation. **Konstantinos Iordanidis:** Writing — review & editing, Investigation. **Richard Taubert:** Writing — review & editing, Supervision, Methodology. **Heiner Wedemeyer:** Writing — review & editing, Supervision. **Fatih Noyan:** Writing — review & editing, Supervision. **Matthias Hardtke-Wolenski:** Writing — review & editing, Supervision, Project administration, Conceptualization. **Elmar Jaeckel:** Writing — review & editing, Supervision, Funding acquisition, Conceptualization.

FUNDING

The authors were supported by grants from the Deutsche Forschungsgemeinschaft (SFB 738, SFB TR127) as well as by the HiLF program (Hochschulinterne Leistungsförderung) of Hannover Medical School. Katharina Hupa-Breier and Heiko Schenk were supported by the PRACTIS — Clinician Scientist Program of Hannover Medical School, funded by the German Research Foundation (DFG, ME 3696/3-1). The funders had no influence on study design, data collection and analysis, decision to publish or preparation of the manuscript.

DECLARATION OF COMPETING INTEREST

Katharina Hupa-Breier received Honoria and travel support from Falk Pharma, Eli Lilly GmBH and NovoNordisk.

Heiko Schenk received Honoria and travel support from GSK, AstraZeneca and Otsuka Pharma.

Christoph Terkamp received honoraria and travel support from AstraZeneca, Boehringer Ingelheim, Lilly, Novo Nordisk, Pfizer and Sandoz.

Elmar Jaeckel has received honoraria and travel support from Eli Lilly GmbH and Boehringer Ingelheim.

M. P. Manns received honoria, travel support and grants from Gilead and Falk Pharma. He acts as principal investigator and consultant for Novartis, Aram Chol, Gilead, Intercept, Falk Pharma and Genfit.
Heiner Wedemeyer received lecture fees from Falk Pharma, Gore, Merz and Norgine and acts as a Principal Investigator for Falk Pharma. He received grants from Merz and Norgine.
These activities do not relate to the current manuscript which was done without any support from the above mentioned companies.
All other authors declare no conflicts of Interests.

DATA AVAILABILITY

Data will be made available on request.

INSTITUTIONAL REVIEW BOARD STATEMENT

All animal experiments were executed according to protocols approved by the animal welfare commission of the Hannover Medical School and local Ethics Animal Review Board (Niedersaechsisches Landesamt für Verbraucherschutz und Lebensmittelsicherheit/LAVES, Oldenburg, Germany) covered by study number 17/2456 and are in accordance to the ARRIVE guidelines.

APPENDIX A. SUPPLEMENTARY DATA

Supplementary data to this article can be found online at https://doi.org/10.1016/j.molmet.2025.102104.

REFERENCES

[1] Younossi ZM, Kalligeros M, Henry L. Epidemiology of metabolic dysfunction-associated steatotic liver disease. Clin Mol Hepatol 2024. https://doi.org/10.3350/cmh.2024.0431. Published online August 19, 2024.

[2] Riazi K, Azhari H, Charette JH, Underwood FE, King JA, Afshar EE, et al. The prevalence and incidence of NAFLD worldwide: a systematic review and meta-analysis. Lancet Gastroenterol Hepatol 2022;7(9):851–61.

[3] Eslam M, Sanyal AJ, George J, International Consensus P. MAFLD: a consensus-driven proposed nomenclature for metabolic associated fatty liver disease. Gastroenterology 2020;158(7):1999–2014 e1.

[4] Rinella ME, Lazarus JV, Ratziu V, Francque SM, Sanyal AJ, Kanwal F, et al. A multisociety Delphi consensus statement on new fatty liver disease nomenclature. J Hepatol 2023;79(6):1542–56.

[5] Bedi O, Aggarwal S, Trehanpati N, Ramakrishna G, Krishan P. Molecular and pathological events involved in the pathogenesis of diabetes-associated nonalcoholic fatty liver disease. J Cli Exp Hepatol 2019;9(5):607–18.

[6] Hagström H, Tynelius P, Rasmussen F. High BMI in late adolescence predicts future severe liver disease and hepatocellular carcinoma: a national, population-based cohort study in 1.2 million men. Gut 2018;67(8):1536–42.

[7] Hagström H, Shang Y, Hegmar H, Nasr P. Natural history and progression of metabolic dysfunction-associated steatotic liver disease. Lancet Gastroenterol Hepatol 2024;9(10):944–56.

[8] Ibrahim SH, Hirsova P, Malhi H, Gores GJ. Animal models of nonalcoholic steatohepatitis: eat, delete, and inflame. Dig Dis Sci 2016;61(5):1325–36.

[9] Cho YR, Kim HJ, Park SY, Ko HJ, Hong EG, Higashimori T, et al. Hyperglycemia, maturity-onset obesity, and insulin resistance in NONcNZO10/LtJ males, a new mouse model of type 2 diabetes. Am J Physiol Endocrinol Metabol 2007;293(1):E327–36.

[10] Kim JH, Saxton AM. The TALLYHO mouse as a model of human type 2 diabetes. Methods Mol Biol 2012;933:75–87.

[11] Denvir J, Boskovic G, Fan J, Primerano DA, Parkman JK, Kim JH. Whole genome sequence analysis of the TALLYHO/Jng mouse. BMC Genom 2016;17(1):907.

[12] Tacke F, Canbay A, Bantel H, Bojunga J, de Laffolie J, Demir JM, et al. Updated S2k clinical practice guideline on non-alcoholic fatty liver disease (NAFLD) issued by the German society of gastroenterology, digestive and metabolic diseases (DGVS) – April 2022 – AWMF registration No.: 021–025. Zeitschrift fur Gastroenterol 2022;60(9):e733–801.

[13] Colosimo S, Tan GD, Petroni ML, Marchesini G, Tomlinson JW. Improved glycaemic control in patients with type 2 diabetes has a beneficial impact on NAFLD, independent of change in BMI or glucose lowering agent. Nutr Metabol Cardiovasc Dis 2023;33(3):640–8.

[14] DeFronzo RA. Combination therapy with GLP-1 receptor agonist and SGLT2 inhibitor. Diabetes Obes Metabol 2017;19(10):1353–62.

[15] DeFronzo RA, Norton L, Abdul-Ghani M. Renal, metabolic and cardiovascular considerations of SGLT2 inhibition. Nat Rev Nephrol 2017;13(1):11–26.

[16] Kahl S, Gancheva S, Straßburger K, Herder C, Machann J, Katsuyama H, et al. Empagliflozin effectively lowers liver fat content in well-controlled type 2 diabetes: a randomized, double-blind, phase 4, placebo-controlled trial. Diabetes Care 2019;43(2):298–305.

[17] Mao X, Zhang X, Kam L, Chien N, Lai R, Cheung KS, et al. Synergistic association of sodium-glucose cotransporter-2 inhibitor and metformin on liver and non-liver complications in patients with type 2 diabetes mellitus and metabolic dysfunction-associated steatotic liver disease. Gut 2024;73(12):2054–61.

[18] Kawaguchi T, Murotani K, Kajiyama H, Obara H, Yamaguchi H, Toyofuku Y, et al. Effects of luseogliflozin on suspected MASLD in patients with diabetes: a pooled meta-analysis of phase III clinical trials. J Gastroenterol 2024;59(9):836–48.

[19] Shen TH, Aby ES, Vock D, Farley JF. Sodium-glucose co-transporter-2 inhibitors versus dipeptidyl peptidase-4 inhibitors on major liver outcomes in metabolic dysfunction-associated steatotic liver disease. Diabetes Obes Metabol 2024;26(11):5116–25.

[20] Diaz Marin R, Crespo-Garcia S, Wilson AM, Sapieha P. RELi protocol: optimization for protein extraction from white, brown and beige adipose tissues. MethodsX 2019;6:918–28.

[21] Hardtke-Wolenski M, Fischer K, Noyan F, Schlue J, Falk CS, Stahlhut M, et al. Genetic predisposition and environmental danger signals initiate chronic autoimmune hepatitis driven by CD4+ T cells. Hepatology 2013;58(2):718–28.

[22] Franko A, Neschen S, Rozman J, Rathkolb B, Aichler M, Feuchtinger A, et al. Bezafibrate ameliorates diabetes via reduced steatosis and improved hepatic insulin sensitivity in diabetic TallyHo mice. Mol Metabol 2017;6(3):256–66.

[23] Kleiner DE, Brunt EM, Van Natta M, Behling C, Contos MJ, Cummings OW, et al. Design and validation of a histological scoring system for nonalcoholic fatty liver disease. Hepatology 2005;41(6):1313–21.

[24] Schindelin J, Arganda-Carreras I, Frise E, Kaynig V, Longair M, Pietzsch T, et al. Fiji: an open-source platform for biological-image analysis. Nat Methods 2012;9(7):676–82.

[25] Endig J, Buitrago-Molina LE, Marhenke S, Reisinger F, Saborowski A, Schütt J, et al. Dual role of the adaptive immune system in liver injury and hepatocellular carcinoma development. Cancer Cell 2016;30(2):308–23.

[26] Heidrich B, Vital M, Plumeier I, Doscher N, Kahl S, Kirschner J, et al. Intestinal microbiota in patients with chronic hepatitis C with and without cirrhosis compared with healthy controls. Liver Int : Official Journal of the International Association for the Study of the Liver 2018;38(1):50–8.

[27] Brown GT, Kleiner DE. Histopathology of nonalcoholic fatty liver disease and nonalcoholic steatohepatitis. Metab, Clin Exp 2016;65(8):1080–6.

[28] Vonderlin J, Chavakis T, Sieweke M, Tacke F. The multifaceted roles of macrophages in NAFLD pathogenesis. Cell Mol Gastroenterol Hepatol 2023;15(6):1311–24.

[29] Rahman K, Vengrenyuk Y, Ramsey SA, Vila NR, Girgis NM, Liu J, et al. Inflammatory Ly6Chi monocytes and their conversion to M2 macrophages drive atherosclerosis regression. J Clin Invest 2017;127(8):2904–15.
[30] Kanehisa M, Sato Y, Kawashima M, Furumichi M, Tanabe M. KEGG as a reference resource for gene and protein annotation. Nucleic Acids Res 2016;44(D1):D457–62.
[31] Marakala V. Neutrophil gelatinase-associated lipocalin (NGAL) in kidney injury - a systematic review. Clin Chim Acta; Int J Clin Chem 2022;536:135–41.
[32] Wen Y, Parikh CR. Current concepts and advances in biomarkers of acute kidney injury. Crit Rev Clin Lab Sci 2021;58(5):354–68.
[33] Ong Lopez AMC, Pajimna JAT. Efficacy of sodium glucose cotransporter 2 inhibitors on hepatic fibrosis and steatosis in non-alcoholic fatty liver disease: an updated systematic review and meta-analysis. Sci Rep 2024;14(1):2122.
[34] Im YR, Hunter H, de Gracia Hahn D, Duret A, Cheah Q, Dong J, et al. A systematic review of animal models of NAFLD finds high-fat, high-fructose diets most closely resemble human NAFLD. Hepatology 2021;74(4):1884–901.
[35] Meijnikman AS, Fondevila MF, Arrese M, Kisseleva T, Bataller R, Schnabl B. Towards more consistent models and consensual terminology in preclinical research for Steatotic Liver Disease. J Hepatol 2024.
[36] Kanwar P, Kowdley KV. The metabolic syndrome and its influence on nonalcoholic steatohepatitis. Clin Liver Dis 2016;20(2):225–43.
[37] Kim JH, Stewart TP, Zhang W, Kim HY, Nishina PM, Naggert JK. Type 2 diabetes mouse model TallyHo carries an obesity gene on chromosome 6 that exaggerates dietary obesity. Physiol Genom 2005;22(2):171–81.
[38] Asgharpour A, Cazanave SC, Pacana T, Seneshaw M, Vincent R, Banini BA, et al. A diet-induced animal model of non-alcoholic fatty liver disease and hepatocellular cancer. J Hepatol 2016;65(3):579–88.
[39] Teufel A, Itzel T, Erhart W, Brosch M, Wang XY, Kim YO, et al. Comparison of gene expression patterns between mouse models of nonalcoholic fatty liver disease and liver tissues from patients. Gastroenterology 2016;151(3):513–525.e0.
[40] Machado MV, Diehl AM. Pathogenesis of nonalcoholic steatohepatitis. Gastroenterology 2016;150(8):1769–77.
[41] Huebbe P, Bilke S, Rueter J, Schloesser A, Campbel G, Glüer CC, et al. Human APOE4 protects high-fat and high-sucrose diet fed targeted replacement mice against fatty liver disease compared to APOE3. Aging Dis 2024;15(1):259–81.
[42] Moreno-Vedia J, Girona J, Ibarretxe D, Masana L, Rodriguez-Calvo R. Unveiling the role of the fatty acid binding protein 4 in the metabolic-associated fatty liver disease. Biomedicines 2022;10(1).
[43] Coilly A, Desterke C, Guettier C, Samuel D, Chiappini F. FABP4 and MMP9 levels identified as predictive factors for poor prognosis in patients with nonalcoholic fatty liver using data mining approaches and gene expression analysis. Sci Rep 2019;9(1):19785.
[44] Miquilena-Colina ME, Lima-Cabello E, Sanchez-Campos S, Garcia-Mediavilla MV, Fernandez-Bermejo M, Lozano-Rodriguez T, et al. Hepatic fatty acid translocase CD36 upregulation is associated with insulin resistance, hyperinsulinaemia and increased steatosis in non-alcoholic steatohepatitis and chronic hepatitis C. Gut 2011;60(10):1394–402.
[45] Wilson CG, Tran JL, Erion DM, Vera NB, Febbraio M, Weiss EJ. Hepatocyte-Specific disruption of CD36 attenuates fatty liver and improves insulin sensitivity in HFD-fed mice. Endocrinology 2016;157(2):570–85.
[46] Rada P, Gonzalez-Rodriguez A, Garcia-Monzon C, Valverde AM. Understanding lipotoxicity in NAFLD pathogenesis: is CD36 a key driver? Cell Death Dis 2020;11(9):802.
[47] Tsai TH, Chen E, Li L, Saha P, Lee HJ, Huang LS, et al. The constitutive lipid droplet protein PLIN2 regulates autophagy in liver. Autophagy 2017;13(7):1130–44.
[48] Najt CP, Senthivinayagam S, Aljazi MB, Fader KA, Olenic SD, Brock JR, et al. Liver-specific loss of Perilipin 2 alleviates diet-induced hepatic steatosis, inflammation, and fibrosis. Am J Physiol Gastrointest Liver Physiol 2016;310(9):G726–38.
[49] Nagaya T, Tanaka N, Suzuki T, Sano K, Horiuchi A, Komatsu M, et al. Down-regulation of SREBP-1c is associated with the development of burned-out NASH. J Hepatol 2010;53(4):724–31.
[50] Wang Q, Chang B, Li X, Zou Z. Role of ALDH2 in hepatic disorders: gene polymorphism and disease pathogenesis. J Clin Transl Hepatol 2021;9(1):90–8.
[51] Kendall TJ, Jimenez-Ramos M, Turner F, Ramachandran P, Minnier J, McColgan MD, et al. An integrated gene-to-outcome multimodal database for metabolic dysfunction-associated steatotic liver disease. Nat Med 2023;29(11):2939–53.
[52] Koliaki C, Szendroedi J, Kaul K, Jelenik T, Nowotny P, Jankowiak F, et al. Adaptation of hepatic mitochondrial function in humans with non-alcoholic fatty liver is lost in steatohepatitis. Cell Metabol 2015;21(5):739–46.
[53] Shin SK, Cho HW, Song SE, Song DK. Catalase and nonalcoholic fatty liver disease. Pflueg Arch Eur J Physiol 2018;470(12):1721–37.
[54] Riordan JD, Nadeau JH. Modeling progressive non-alcoholic fatty liver disease in the laboratory mouse. Mamm Genome : Official Journal of the International Mammalian Genome Society 2014;25(9–10):473–86.
[55] Sutti S, Albano E. Adaptive immunity: an emerging player in the progression of NAFLD. Nat Rev Gastroenterol Hepatol 2020;17(2):81–92.
[56] Tsouka S, Kumar P, Seubnooch P, Freiburghaus K, St-Pierre M, Dufour JF, et al. Transcriptomics-driven metabolic pathway analysis reveals similar alterations in lipid metabolism in mouse MASH model and human. Commun Med 2024;4(1):39.
[57] Farrell G, Schattenberg JM, Leclercq I, Yeh MM, Goldin R, Teoh N, et al. Mouse models of nonalcoholic steatohepatitis: toward optimization of their relevance to human nonalcoholic steatohepatitis. Hepatology 2019;69(5):2241–57.
[58] Li YY, Zheng TL, Xiao SY, Wang P, Yang WJ, Jiang LL, et al. Hepatocytic ballooning in non-alcoholic steatohepatitis: dilemmas and future directions. Liver Int : Official Journal of the International Association for the Study of the Liver 2023;43(6):1170–82.
[59] Raverdy V, Tavaglione F, Chatelain E, Caiazzo R, Saponaro C, Lassailly G, et al. Performance of non-invasive tests for liver fibrosis resolution after bariatric surgery. Metab, Clin Exp 2024;153:155790.
[60] Lee Y, Doumouras AG, Yu J, Brar K, Banfield L, Gmora S, et al. Complete resolution of nonalcoholic fatty liver disease after bariatric surgery: a systematic review and meta-analysis. Clin Gastroenterol Hepatol : The Official Clinical Practice Journal of the American Gastroenterological Association 2019;17(6):1040–1060 e11.
[61] Dai X, Zheng HL, Ma YX, Wang YY, Wang MQ, Cai HY, et al. Single-cell transcriptome analysis identified Core genes and transcription factors in mesenchymal cell differentiation during liver cirrhosis. Front Biosci 2024;29(2):62.
[62] Krenkel O, Puengel T, Govaere O, Abdallah AT, Mossanen JC, Kohlhepp M, et al. Therapeutic inhibition of inflammatory monocyte recruitment reduces steatohepatitis and liver fibrosis. Hepatology 2018;67(4):1270–83.
[63] Rau M, Schilling AK, Meertens J, Hering I, Weiss J, Jurowich C, et al. Progression from nonalcoholic fatty liver to nonalcoholic steatohepatitis is marked by a higher frequency of Th17 cells in the liver and an increased Th17/resting regulatory T cell ratio in peripheral blood and in the liver. J Immunol 2016;196(1):97–105.
[64] Wang H, Zhang H, Wang Y, Brown ZJ, Xia Y, Huang Z, et al. Regulatory T-cell and neutrophil extracellular trap interaction contributes to carcinogenesis in non-alcoholic steatohepatitis. J Hepatol 2021;75(6):1271–83.
[65] Ma C, Kesarwala AH, Eggert T, Medina-Echeverz J, Kleiner DE, Jin P, et al. NAFLD causes selective CD4(+) T lymphocyte loss and promotes hepatocarcinogenesis. Nature 2016;531(7593):253–7.
[66] Dudek M, Pfister D, Donakonda S, Filpe P, Schneider A, Laschinger M, et al. Auto-aggressive CXCR6+ CD8 T cells cause liver immune pathology in NASH. Nature 2021;592(7854):444–9.
[67] Nati M, Haddad D, Birkenfeld AL, Koch CA, Chavakis T, Chatzigeorgiou A. The role of immune cells in metabolism-related liver inflammation and

development of non-alcoholic steatohepatitis (NASH). Rev Endocr Metab Disord 2016;17(1):29—39.
[68] Deng CJ, Lo TH, Chan KY, Li X, Wu MY, Xiang Z, et al. Role of B Lymphocytes in the pathogenesis of NAFLD: a 2022 update. Int J Mol Sci 2022;23(20).
[69] Safari Z, Gerard P. The links between the gut microbiome and non-alcoholic fatty liver disease (NAFLD). Cell Mol Life Sci : CMLS 2019;76(8):1541—58.
[70] Tilg H, Cani PD, Mayer EA. Gut microbiome and liver diseases. Gut 2016;65(12):2035—44.
[71] Quesada-Vazquez S, Aragones G, Del Bas JM, Escote X. Diet, gut microbiota and non-alcoholic fatty liver disease: three parts of the same Axis. Cells 2020;9(1).
[72] Loomba R, Seguritan V, Li W, Long T, Klitgord N, Bhatt A, et al. Gut microbiome-based metagenomic signature for non-invasive detection of advanced fibrosis in human nonalcoholic fatty liver disease. Cell Metabol 2017;25(5):1054—10562 e5.
[73] Del Chierico F, Nobili V, Vernocchi P, Russo A, De Stefanis C, Gnani D, et al. Gut microbiota profiling of pediatric nonalcoholic fatty liver disease and obese patients unveiled by an integrated meta-omics-based approach. Hepatology 2017;65(2):451—64.
[74] Gomez-Zorita S, Aguirre L, Milton-Laskibar I, Fernandez-Quintela A, Trepiana J, Kajarabille N, et al. Relationship between changes in microbiota and liver steatosis induced by high-fat feeding-A review of rodent models. Nutrients 2019;11(9).
[75] Bissig-Choisat B, Alves-Bezerra M, Zorman B, Ochsner SA, Barzi M, Legras X, et al. A human liver chimeric mouse model for non-alcoholic fatty liver disease. JHEP Rep 2021;3(3).
[76] Giles DA, Moreno-Fernandez ME, Stankiewicz TE, Graspeuntner S, Cappelletti M, Wu D, et al. Thermoneutral housing exacerbates nonalcoholic fatty liver disease in mice and allows for sex-independent disease modeling. Nat Med 2017;23(7):829—38.
[77] Brummer C, Singer K, Brand A, Bruss C, Renner K, Herr W, et al. Sex-dependent T cell dysregulation in mice with diet-induced obesity. Int J Mol Sci 2024;25(15).
[78] Byrne CD, Targher G. NAFLD as a driver of chronic kidney disease. J Hepatol 2020;72(4):785—801.
[79] Fede G, D'Amico G, Arvaniti V, Tsochatzis E, Germani G, Georgiadis D, et al. Renal failure and cirrhosis: a systematic review of mortality and prognosis. J Hepatol 2012;56(4):810—8.
[80] Sun DQ, Jin Y, Wang TY, Zheng KI, Rios RS, Zhang HY, et al. MAFLD and risk of CKD. Metab, Clin Exp 2021;115:154433.
[81] Deji N, Kume S, Araki S, Soumura M, Sugimoto T, Isshiki K, et al. Structural and functional changes in the kidneys of high-fat diet-induced obese mice. Am J Physiol Ren Physiol 2009;296(1):F118—26.
[82] Kashani K, Cheungpasitporn W, Ronco C. Biomarkers of acute kidney injury: the pathway from discovery to clinical adoption. Clin Chem Lab Med 2017;55(8):1074—89.
[83] Navarro-Gonzalez JF, Mora-Fernandez C. The role of inflammatory cytokines in diabetic nephropathy. J Am Soc Nephrol 2008;19(3):433—42.
[84] Kelly KJ, Liu Y, Zhang J, Dominguez JH. Renal C3 complement component: feed forward to diabetic kidney disease. Am J Nephrol 2015;41(1):48—56.
[85] Lei Y, Devarapu SK, Motrapu M, Cohen CD, Lindenmeyer MT, Moll S, et al. Interleukin-1beta inhibition for chronic kidney disease in obese mice with type 2 diabetes. Front Immunol 2019;10:1223.
[86] Mezzano S, Aros C, Droguett A, Burgos ME, Ardiles L, Flores C, et al. NF-kappaB activation and overexpression of regulated genes in human diabetic nephropathy. Nephrol Dial Transplant 2004;19(10):2505—12.
[87] Vacca M, Kamzolas I, Harder LM, Oakley F, Trautwein C, Hatting M, et al. An unbiased ranking of murine dietary models based on their proximity to human metabolic dysfunction-associated steatotic liver disease (MASLD). Nat Metab 2024;6(6):1178—96.
[88] Hebbard L, George J. Animal models of nonalcoholic fatty liver disease. Nat Rev Gastroenterol Hepatol 2011;8(1):35—44.
[89] Geidl-Flueck B, Gerber PA. Fructose drives de novo lipogenesis affecting metabolic health. J Endocrinol 2023.
[90] Al-Humadi H, Theocharis S, Dontas I, Stolakis V, Zarros A, Kyriakaki A, et al. Hepatic injury due to combined choline-deprivation and thioacetamide administration: an experimental approach to liver diseases. Dig Dis Sci 2012;57(12):3168—77.
[91] Saxena R, Nassiri M, Yin X-M, Morral N. Insights from a high-fat diet fed mouse model with a humanized liver. PLoS One 2022;17(5):e0268260.
[92] Tozzi M, Feigh M, Hansen HH. 1642-P: metabolic effects of semaglutide and Resmetirom at thermoneutrality in the diet-induced obese mouse. Diabetes 2024;73(Supplement_1).
[93] Harrison SA, Taub R, Neff GW, Lucas KJ, Labriola D, Moussa SE, et al. Resmetirom for nonalcoholic fatty liver disease: a randomized, double-blind, placebo-controlled phase 3 trial. Nat Med 2023;29(11):2919—28.
[94] Loomba R, Abdelmalek MF, Armstrong MJ, Jara M, Kjær MS, Krarup N, et al. Semaglutide 2·4 mg once weekly in patients with non-alcoholic steatohepatitis-related cirrhosis: a randomised, placebo-controlled phase 2 trial. Lancet Gastroenterol Hepatol 2023;8(6):511—22.
[95] Brown E, Heerspink HJL, Cuthbertson DJ, Wilding JPH. SGLT2 inhibitors and GLP-1 receptor agonists: established and emerging indications. Lancet 2021;398(10296):262—76.
[96] Cheung KS, Ng HY, Hui RWH, Lam LK, Mak LY, Ho YC, et al. Effects of empagliflozin on liver fat in patients with metabolic dysfunction-associated steatotic liver disease without diabetes mellitus: a randomized, double-blind, placebo-controlled trial. Hepatology 2024;80(4):916—27.
[97] Kuchay MS, Krishan S, Mishra SK, Farooqui KJ, Singh MK, Wasir JS, et al. Effect of empagliflozin on liver fat in patients with type 2 diabetes and nonalcoholic fatty liver disease: a randomized controlled trial (E-LIFT trial). Diabetes Care 2018;41(8):1801—8.
[98] Hupa-Breier KL, Dywicki J, Hartleben B, Wellhoner F, Heidrich B, Taubert R, et al. Dulaglutide alone and in combination with empagliflozin attenuate inflammatory pathways and microbiome dysbiosis in a non-diabetic mouse model of NASH. Biomedicines 2021;9(4).
[99] Androutsakos T, Nasiri-Ansari N, Bakasis AD, Kyrou I, Efstathopoulos E, Randeva HS, et al. SGLT-2 inhibitors in NAFLD: expanding their role beyond diabetes and cardioprotection. Int J Mol Sci 2022;23(6).
[100] Tsai KF, Chen YL, Chiou TT, Chu TH, Li LC, Ng HY, et al. Emergence of SGLT2 inhibitors as powerful antioxidants in human diseases. Antioxidants 2021;10(8).
[101] Vairetti M, Di Pasqua LG, Cagna M, Richelmi P, Ferrigno A, Berardo C. Changes in glutathione content in liver diseases: an update. Antioxidants 2021;10(3):364.
[102] Wang Y, Ding Y, Sun P, Zhang W, Xin Q, Wang N, et al. Empagliflozin-enhanced antioxidant defense attenuates lipotoxicity and protects hepatocytes by promoting FoxO3a- and Nrf2-mediated nuclear translocation via the CAMKK2/AMPK pathway. Antioxidants 2022;11(5).
[103] Liu W, You D, Lin J, Zou H, Zhang L, Luo S, et al. SGLT2 inhibitor promotes ketogenesis to improve MASH by suppressing CD8+ T cell activation. Cell Metabol 2024;36(10):2245. -61.e6.

